Erin E. Mulvihill,[1] Elodie M. Varin,[1] John R. Ussher,[1] Jonathan E. Campbell,[1] K.W. Annie Bang,[1] Tahmid Abdullah,[1] Laurie L. Baggio,[1] and Daniel J. Drucker[1,2]

Inhibition of Dipeptidyl Peptidase-4 Impairs Ventricular Function and Promotes Cardiac Fibrosis in High Fat–Fed Diabetic Mice

Diabetes 2016;65:742–754 | DOI: 10.2337/db15-1224

PATHOPHYSIOLOGY

Dipeptidyl peptidase-4 (DPP4) inhibitors used for the treatment of type 2 diabetes are cardioprotective in preclinical studies; however, some cardiovascular outcome studies revealed increased hospitalization rates for heart failure (HF) among a subset of DPP4 inhibitor–treated subjects with diabetes. We evaluated cardiovascular function in young euglycemic *Dpp4*$^{-/-}$ mice and in older, high fat–fed, diabetic C57BL/6J mice treated with either the glucagon-like peptide 1 receptor (GLP-1R) agonist liraglutide or the highly selective DPP4 inhibitor MK-0626. We assessed glucose metabolism, ventricular function and remodeling, and cardiac gene expression profiles linked to inflammation and fibrosis after transverse aortic constriction (TAC) surgery, a pressure-volume overload model of HF. Young euglycemic *Dpp4*$^{-/-}$ mice exhibited a cardioprotective response after TAC surgery or doxorubicin administration, with reduced fibrosis; however, cardiac mRNA analysis revealed increased expression of inflammation-related transcripts. Older, diabetic, high fat–fed mice treated with the GLP-1R agonist liraglutide exhibited preservation of cardiac function. In contrast, diabetic mice treated with MK-0626 exhibited modest cardiac hypertrophy, impairment of cardiac function, and dysregulated expression of genes and proteins controlling inflammation and cardiac fibrosis. These findings provide a model for the analysis of mechanisms linking fibrosis, inflammation, and impaired ventricular function to DPP4 inhibition in preclinical studies.

Patients with type 2 diabetes are at increased risk for the development of cardiovascular disease (CVD) (1,2), including peripheral vascular disease, coronary artery disease, and heart failure (HF) (3). Although the use of antidiabetic agents to lower glycemia results in the reduction of microvascular disease, the rates of macrovascular disease remain elevated and take much longer to decline with glucose-lowering therapies. Heightened concern over the possible cardiovascular side effects of thiazolidinediones, notably rosiglitazone, prompted the development of regulatory guidance for evaluation of the cardiovascular safety of glucose-lowering agents (4). Hence, sponsors now carry out large cardiovascular outcome studies in subjects with diabetes who have established CVD or are at high risk for CVD.

Two classes of antidiabetic agents, designated incretin therapies, exert their glucoregulatory effects through the potentiation of gut hormone action (5). Dipeptidyl peptidase-4 inhibitors (DPP4is) control glycemia by preventing the degradation of glucagon-like peptide 1 (GLP-1) and glucose-dependent insulinotropic polypeptide, resulting in the stimulation of insulin and inhibition of glucagon secretion. GLP-1 receptor (GLP-1R) agonists potentiate GLP-1R signaling, leading to increased insulin levels; reduced glucagon secretion, gastric emptying, and appetite; and modest weight loss. Dozens of preclinical studies (6,7) have demonstrated that incretin therapies reduce atherosclerosis and vascular injury, decrease inflammation, and are cardioprotective in experimental models of

[1]Lunenfeld-Tanenbaum Research Institute, Mount Sinai Hospital, Toronto, Ontario, Canada
[2]Department of Medicine, University of Toronto, Toronto, Ontario, Canada
Corresponding author: Daniel J. Drucker, drucker@lunenfeld.ca.

Received 2 September 2015 and accepted 7 December 2015.
This article contains Supplementary Data online at http://diabetes.diabetesjournals.org/lookup/suppl/doi:10.2337/db15-1224/-/DC1.

E.E.M., E.M.V., and J.R.U. contributed equally to this article and are co–first authors.

J.R.U. is currently affiliated with the Faculty of Pharmacy and Pharmaceutical Sciences, University of Alberta, Edmonton, Alberta, Canada.

CVD. Furthermore, incretin therapies reduce blood pressure and decrease postprandial lipemia in subjects with type 2 diabetes and exert cardioprotective actions in short-term clinical studies (6,7). Moreover, meta-analyses of clinical trials (6,7) in subjects with diabetes without established CVD suggest that these agents may reduce cardiovascular event rates.

Conversely, outcome studies (8–10) have demonstrated cardiovascular safety, but no evidence for the reduction of cardiovascular event rates, with three different DPP4is, saxagliptin, alogliptin, and sitagliptin. Unexpectedly, subjects treated with saxagliptin in the Saxagliptin Assessment of Vascular Outcomes Recorded in Patients with Diabetes Mellitus—Thrombolysis in Myocardial Infarction 53 (SAVOR-TIMI 53) study exhibited a small but significant increase in the rate of hospitalization for HF (9). Furthermore, patients receiving alogliptin in the Examination of Cardiovascular Outcomes with Alogliptin versus Standard of Care (EXAMINE) trial exhibited a small numeric excess of HF events (10,11).

We have now examined the cardiovascular responses of younger *Dpp4*$^{-/-}$ mice and older, dysglycemic, high fat–fed mice after transverse aortic constriction (TAC) induction of experimental HF. Genetic reduction of DPP4 activity was cardioprotective in euglycemic *Dpp4*$^{-/-}$ mice with experimental TAC-induced HF. In contrast, pharmacological DPP4 inhibition was not cardioprotective in older, dysglycemic, dyslipidemic mice. Unexpectedly, we detected evidence for increased inflammation in *Dpp4*$^{-/-}$ hearts, and gene expression profiles consistent with both inflammation and fibrosis in hearts from mice treated with a selective DPP4i. Collectively, these findings reveal that DPP4 inhibition is not uniformly cardioprotective in animal studies and provide an experimental model for ongoing analysis of how the reduction of DPP4 activity may promote cardiac fibrosis and inflammation and impair ventricular function in preclinical studies of HF.

RESEARCH DESIGN AND METHODS

Animals, Reagents, and Diets

Mice were housed under a 12-h light/dark cycle in the Toronto Centre for Phenogenomics facility and maintained on chow (Teklad 2018 [18% kcal from fat]; Harlan, Mississauga, Ontario, Canada) with free access to food and water, unless otherwise noted. *Dpp4*$^{-/-}$ mice (Supplementary Fig. 1) were described previously (12); for doxorubicin experiments, n = 4–12 mice per group for vehicle controls and 9–12 mice per group for doxorubicin treatment. For TAC studies in *Dpp4*$^{+/+}$ vs. *Dpp4*$^{-/-}$ vs. mice, n = 6–7 per group. All experiments (Supplementary Fig. 2) used age- and sex-matched littermates. C57BL/6J mice were from The Jackson Laboratory (Bar Harbor, ME). Male C57BL/6J mice, 8–12 weeks of age, were housed two to three per cage and were fed ad libitum for 12 weeks (n = 12–15/group) with a high-fat diet (HFD) (45% kcal fat, 35% kcal carbohydrate, 0.05% w/w cholesterol; catalog #D12451; Research Diets). After 12 weeks of HFD feeding, mice were fasted for 5 h and injected with a single dose of streptozotocin (STZ) (90 mg/kg i.p., freshly prepared solution in 0.1 mmol/L sodium citrate, pH 5.5). One week later, mice were stratified by glucose and body weight and were randomized to three groups that were all maintained on the HFD. Two groups were injected once daily with either saline or liraglutide (30 μg/kg; Novo Nordisk). A third group was administered the DPP4i MK-0626, (2S,3S)-1-(3,3-difluropyrrolidin-1-yl)-4-(dimethylamino)-1,4-dioxo-3-(4-[1,2,4]triazolo[1,5-A]pyridin-6-ylphenyl) butan-2-aminium chloride, designated compound 6b in the study by Edmondson et al. (13), mixed into the HFD (18 mg/kg diet or 3 mg/kg body wt; Merck Laboratories, Rahway, NJ) and also injected daily with saline solution. MK-0626 is from a related yet different structural class than sitagliptin or des-fluoro-sitagliptin (13). We chose to use MK-0626 because it is a highly selective α-amino amide–derived DPP4i (13) previously used for the analysis of cardiac function in rodents (14). Doses of MK-0626 and liraglutide were based on pilot studies (13,15) to achieve equivalent glucose control without reduction of food intake or body weight. Mice were fasted for 4 h prior to sacrifice. All experiments were approved by the Animal Care and Use Subcommittee at the Toronto Centre for Phenogenomics, Mount Sinai Hospital.

TAC Surgery

Buprenorphine was administered 1 h preemptively (0.1 mg/kg s.c.) and every 12 h for 3 days after surgery. Mice were anesthetized with 3% isoflurane and intubated via insertion of a 20-gauge intravenous catheter attached to a connector into the trachea. The transverse aortic arch was banded between the innominate artery and the left common carotid artery with a 27-gauge (diabetic C57BL/6J mice) or 28-gauge (*Dpp4*$^{+/+}$and *Dpp4*$^{-/-}$) needle using 7–0 silk suture. Sham-operated mice underwent the same procedure by moving the suture behind the transverse aortic arch but without tying it off.

Physiological Measurements

Heart rate was assessed via implanted radiotelemetry devices (PA-C10; DSI) (16). Blood pressure was assessed in conscious mice using the CODA system (Kent Scientific, Torrington, CT) (17). Body composition was assessed by an EchoMRI quantitative nuclear magnetic resonance system (Echo Medical Systems, Houston, TX). Oral glucose tolerance tests were performed after an overnight fast, as previously described (16). Exercise capacity was performed by running animals on a calibrated, motor-driven treadmill (Columbus Instruments), as previously described (18).

Plasma and Tissue Analyses

Mice were killed by injection with avertin, and hearts were frozen in liquid nitrogen–cooled Wollenberger tongs (16). Cardiac blood was collected, and plasma was prepared and stored at −80°C. Tissues were removed, snap frozen in liquid nitrogen, and stored at −80°C. Plasma insulin level (ELISA; ALPCO Diagnostics, Windham, NH), HbA_{1c} level

(DCA 2000+ Analyzer; Bayer, Toronto, Ontario, Canada), DPP4 activity (substrate 10 mmol/L H-Gly-Pro-AMC HBr [catalog #I-1225; BACHEM], standard AMC [catalog #Q-1025; BACHEM]), and active GLP-1 7-36 level (immunogenicity assay; Mesoscale) were determined as per manufacturer instructions. Plasma triglycerides (Roche Diagnostics, Laval, Quebec, Canada) and plasma cholesterol (Wako Chemicals, Richmond, VA) were measured enzymatically (19).

Immunoblot Analysis, Histology, Gene Expression, and Cytokine/Chemokine Analysis

Immunoblotting and histological analysis (a separate cohort n = 3–4) were performed as previously reported (16) using antibodies listed in Supplementary Table 1, with the exception of collagen type 1a1 (Col1a1), which was run under nonreducing and nondenaturing conditions. The heart was processed and cut into three equal sections across a vertical axis. Cardiac morphometry was performed with Aperio ImageScope Viewer software (Leica Biosystems) on all three sections of the heart using digital planimetry. For analysis of trichrome staining, settings were modified such that the Positive Pixel Algorithm was set to a hue value of 0.62, a hue width of 0.40, and a color saturation threshold of 0.005.

Gene expression was performed using primer probe sets manufactured by Applied Biosystems TaqMan Assays-on-Demand (ThermoFisher Scientific) (Supplementary Table 2). Protein levels of MCP-1 (mouse) and transforming growth factor-β1 (TGF-β1) (human) were quantified in heart extracts using Cytometric Bead Array assays (BD Biosciences) (20).

Statistical Analysis

Data are presented as the mean ± SEM. A two-way ANOVA was conducted to test the interaction between surgery/doxorubicin and genotype/treatment, followed by a post hoc Holm-Šidák test or a one-way ANOVA was used with post hoc Tukey test. Statistical analysis was performed using SigmaPlot version 14.0. Data were considered statistically significant at $P \leq 0.05$.

RESULTS

Cardiac Structure and Function Are Improved in *Dpp4*$^{-/-}$ Mice With HF

We first determined that our *Dpp4*$^{-/-}$ mice used for cardiovascular studies retained the originally described (21) metabolic phenotypes of improved glucose tolerance, elevated GLP-1 levels, and reduced DPP4 activity (Supplementary Fig. 1*A–D*), without changes in fasting blood glucose levels (Supplementary Fig. 1*E*). Furthermore, *Dpp4*$^{-/-}$ mice exhibited lower body weights and reduced adipose tissue mass, as previously reported (Supplementary Fig. 1*F* and *G*) (22). An ultrasound echocardiography assessment demonstrated normal baseline myocardial wall dimensions and cardiac function in young *Dpp4*$^{-/-}$ versus *Dpp4*$^{+/+}$ littermate control mice (Supplementary Fig. 1*H–K*).

To ascertain the susceptibility of normoglycemic *Dpp4*$^{-/-}$ mice to the development of HF, we studied mice with *1*) pressure overload–induced hypertrophy via TAC surgery and *2*) chemically induced cardiomyopathy via administration of the antineoplastic agent doxorubicin (Supplementary Fig. 2). TAC surgery was performed at 10–12 weeks of age. We did not observe differences in survival between *Dpp4*$^{-/-}$ and *Dpp4*$^{+/+}$ littermate control mice after TAC surgery; the survival rate was >90%. At 8 weeks post TAC, left ventricular (LV) mass was increased to a greater extent in *Dpp4*$^{+/+}$ vs. *Dpp4*$^{-/-}$ mice (Fig. 1*A*, P = 0.075). The reduction in LV ejection fraction (LVEF) and LV fractional shortening (Fig. 1*B* and *C*) and dilation of the LV cavity (Fig. 1*D–G* and Supplementary Table 3) were significantly greater in *Dpp4*$^{+/+}$ compared with *Dpp4*$^{-/-}$ mice. No differences in lung weight/tibia length ratio (Fig. 1*H*) or cardiac levels of atrial natriuretic peptide (*Nppa*) and B-type natriuretic peptide (*Nppb*) mRNA transcripts (Fig. 1*I* and *J*) were detected after TAC. The preservation of cardiac function in *Dpp4*$^{-/-}$ mice was associated with a significant improvement in distance and time run on a treadmill prior to exhaustion 8 weeks after TAC surgery (Fig. 1*K* and *L*).

After doxorubicin administration, we did not observe differences in survival (≥80% in all groups); however, greater weight loss was observed in *Dpp4*$^{+/+}$ compared with *Dpp4*$^{-/-}$ mice (Supplementary Fig. 3*A*). Doxorubicin significantly decreased heart weight and LV mass (Supplementary Fig. 3*B* and *C*) and reduced heart dimensions (LV systolic dimension [LVDs], LV diastolic dimension [LVDd]) in *Dpp4*$^{+/+}$ mice, but not in *Dpp4*$^{-/-}$ mice (Supplementary Fig. 3*D* and *E*). Significant elevations in the levels of cardiac mRNA transcripts encoding *Nppb*, *Nppa* (Supplementary Fig. 3*F* and *G*), TGF-β2 (*Tgfb2*), matrix metallopeptidase 9 (*Mmp9*), and tissue inhibitor of metalloproteinase 1 (*Timp1*) and diminished levels of *Col1a1* expression were observed in hearts from both *Dpp4*$^{+/+}$ and *Dpp4*$^{-/-}$ mice after doxorubicin treatment (Supplementary Fig. 4*A–D*). Reductions in the phosphorylation of extracellular signal–related kinase (ERK) 1/2 and increased levels of phosphorylated Akt (after doxorubicin) were similar across genotypes (Supplementary Fig. 4*E* and *F*).

Reduction in Cardiac Fibrosis in *Dpp4*$^{-/-}$ Hearts Post TAC Surgery

Masson trichrome staining intensity trended lower, and ventricular protein levels of Col1a1 were significantly decreased in hearts from *Dpp4*$^{-/-}$ mice post TAC surgery (Fig. 2*A* and *B*). No perturbation in fibrosis-related gene expression profiles was detected (Fig. 2*C–G*). Unexpectedly, levels of gene products expressed by cardiac fibroblasts such as vimentin (*Vim*) and the discoidin domain receptor family 2 (*Ddr2*) (Fig. 2*H* and *I*) were increased in hearts of *Dpp4*$^{-/-}$ mice.

Dysregulation of Inflammation-Related Cardiac Gene Expression in *Dpp4*$^{-/-}$ Hearts Post TAC Surgery

Despite improved cardiac function and reduced fibrosis, we detected significant increases in the expression of genes encoding regulators and effectors of the immune

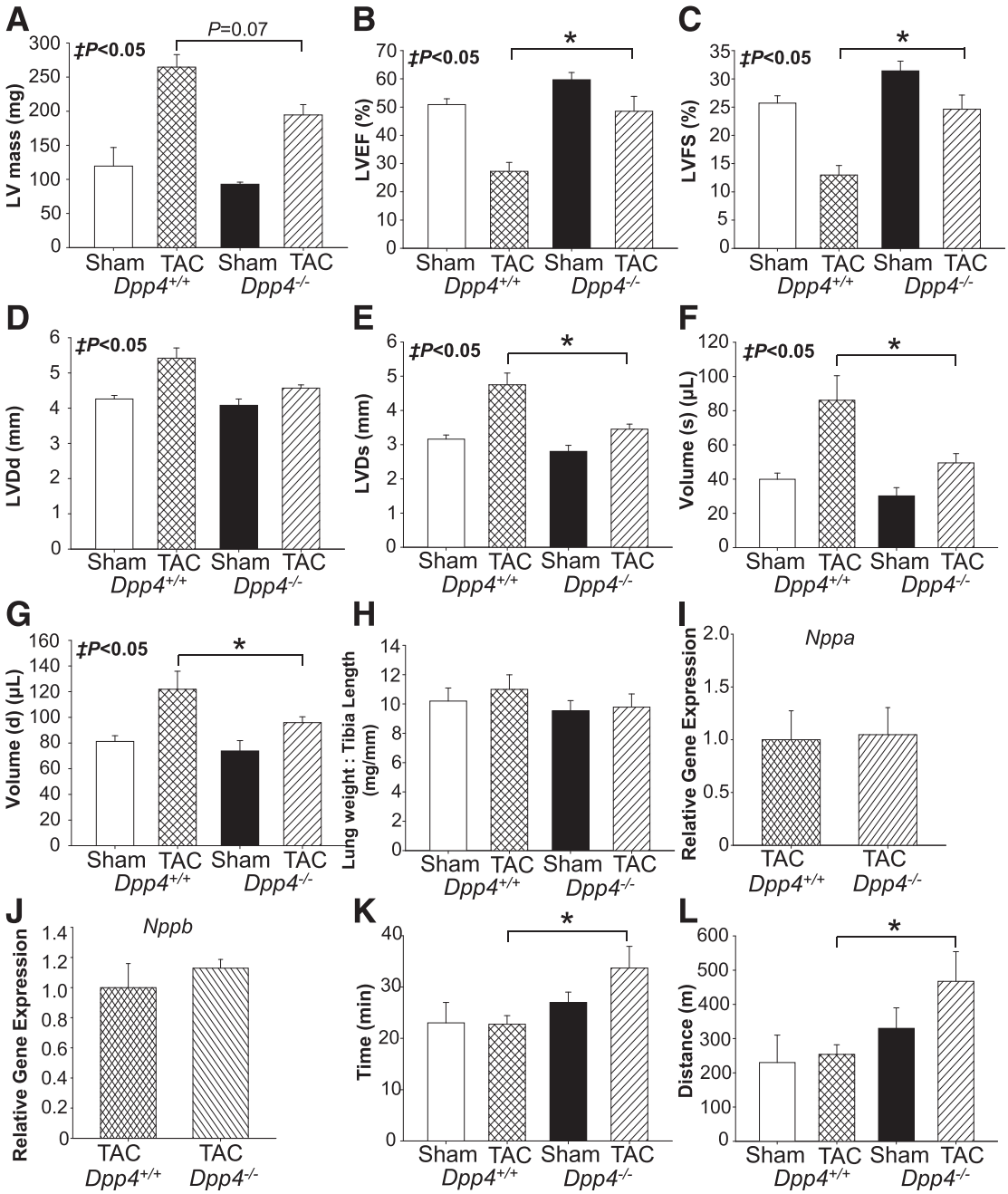

Figure 1—Euglycemic *Dpp4*$^{-/-}$ mice exhibit decreased hypertrophy and preservation of cardiac function in response to pathological pressure overload–induced HF. Echocardiography was performed 8 weeks post TAC surgery, and tissues were harvested 10 weeks after TAC surgery. LV mass (*A*), LVEF (*B*), LV fractional shortening (LVFS) (*C*), LVDd (*D*), LVDs (*E*), systolic volume (*F*), and diastolic volume (*G*) as determined by echocardiography ($n \geq 8$). *H*, Lung weight/tibia length ratio (n = 4–5). *I* and *J*, Relative levels of ventricular mRNA of the hypertrophic markers *Nppa* and *Nppb*. *K* and *L*, Time and distance run on a treadmill prior to exhaustion 8 weeks post TAC surgery. All values are the mean ± SEM (n = 4–5, *$P < 0.05$, ‡$P < 0.05$ sham surgery group vs. TAC surgery group). d, diastolic; s, systolic.

response regulating cardiac inflammation in *Dpp4*$^{-/-}$ mouse hearts, including macrophage chemoattractant proteins 1 and 2 (*Ccl2* and *Ccl8*, respectively), ventricular MCP-1 protein (Fig. 3*A*–*C*), interleukin-1β (*Il1b*), growth differentiation factor 5 (*Gdf5*), and growth differentiation factor 15 (*Gdf15*) (Fig. 3*D*–*F*). No differences were observed for *Tnf* (Fig. 3*G*). Furthermore, *Dpp4*$^{-/-}$ hearts exhibited increased mRNA levels of *1*) the macrophage markers cluster of differentiation (Cd11b-*Itgam*) and *Cd68* (P = 0.06) (Fig. 3*H* and *I*), and *2*) markers of infiltrating hematopoietic cells (*Cd34*) (Fig. 3*J*). Histological staining for CD34 demonstrated increased infiltration of cells of hematopoietic origin in *Dpp4*$^{-/-}$ hearts (Fig. 3*K*). No differences in the expression of hypoxia markers, including heme oxygenase-1 (*Hmox1*), inducible nitric oxide synthase (*Nos2*), endothelial nitric oxide synthase (*Nos3*),

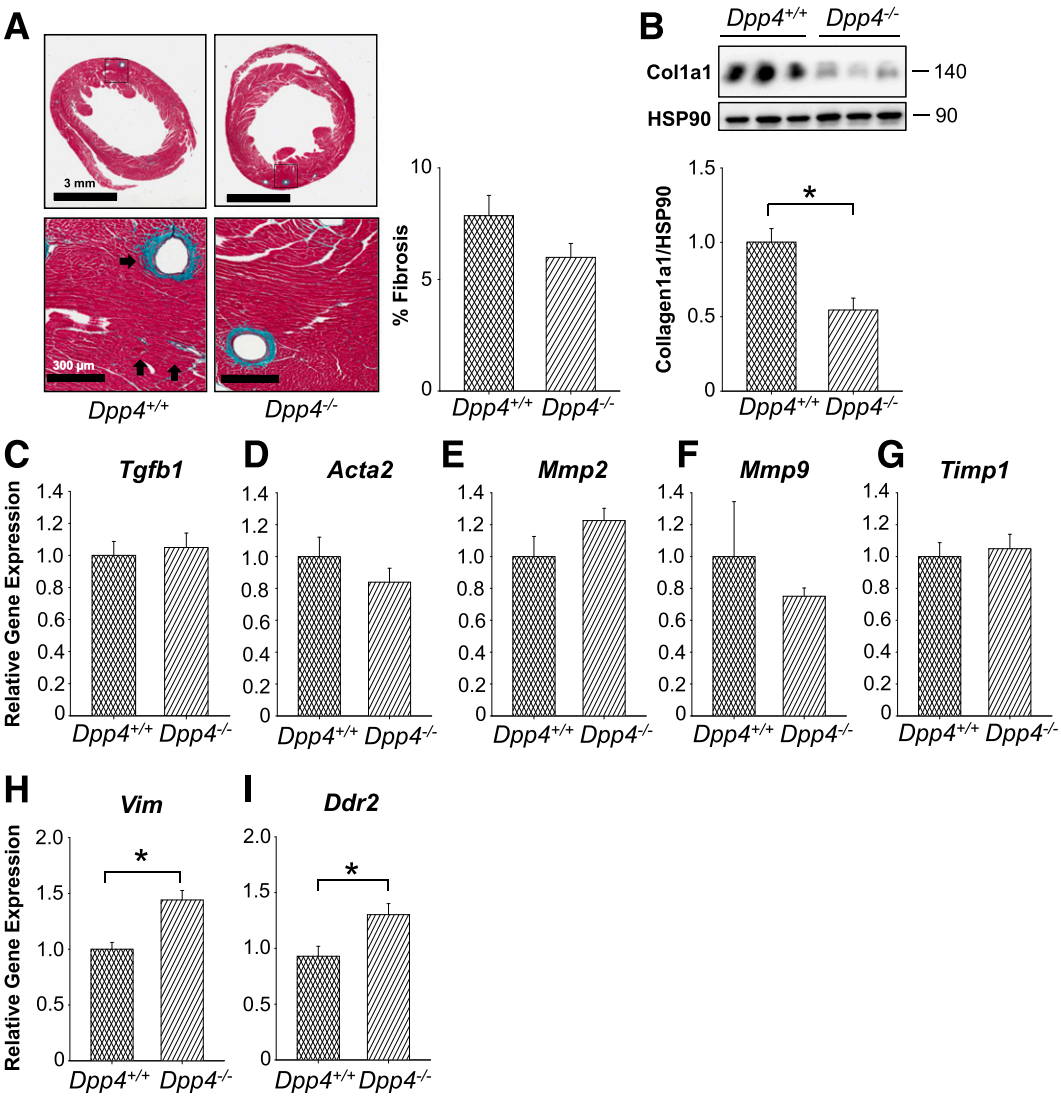

Figure 2—Fibrosis is decreased in euglycemic *Dpp4*$^{-/-}$ mice compared with littermate controls. *A*, Trichrome staining and quantitation of sectioned hearts from *Dpp4*$^{-/-}$ mice compared with littermate controls (n = 4–5). Arrows represent areas of trichrome staining. *B*, Western blotting analysis of Col1a1 normalized to HSP90. Relative levels of ventricular mRNA of the hypertrophic markers *Tgfb1* (*C*), *Acta2* (*D*), *Mmp2* (*E*), *Mmp9* (*F*), *Timp1* (*G*), *Vim* (*H*), and *Ddr2* (*I*). All values are the mean ± SEM (n = 4–5, *P < 0.05).

hypoxia-inducible factor 1α (*Hif1a*), vascular endothelial growth factor α (*Vegfa*), or interleukin-6 (*Il6*) were evident in *Dpp4*$^{-/-}$ versus *Dpp4*$^{+/+}$ hearts (Supplementary Fig. 5*A*–*F*).

Cardiac Structure and Function Are Not Improved After TAC in MK-0626–Treated Diabetic Mice

To verify the selectivity of MK-0626 (13), we performed an oral glucose tolerance test (Supplementary Fig. 6). Glucose excursions were reduced by 50% in *Dpp4*$^{+/+}$ mice, but not in *Dpp4*$^{-/-}$ mice. We next examined the cardiac responses to TAC surgery in HFD-fed mice with low-dose STZ-induced diabetes after prolonged pharmacological DPP4 inhibition or GLP-1R agonism (Supplementary Fig. 2). Mice treated with liraglutide or MK-0626 had improved glucose tolerance, decreased HbA_{1c} and fasting glucose levels, and improved glucose-stimulated insulin levels (Supplementary Fig. 7*A*–*D*). MK-0626 markedly diminished plasma DPP4 activity and increased active GLP-1 levels assessed before and after an oral glucose load (Supplementary Fig. 7*E* and *F*). Plasma triglyceride levels, but not cholesterol levels, were reduced by liraglutide and MK-0626 (Supplementary Fig. 7*G* and *H*). Unexpectedly, mice treated with MK-0626 demonstrated increased body weight (Supplementary Fig. 7), food intake (Supplementary Fig. 7*J*), and fat mass (Supplementary Fig. 7*K* and *L*).

Echocardiography performed 8 weeks post TAC surgery revealed significant increases in LV mass and heart weight only in mice treated with MK-0626 (Fig. 4*A* and *B*); however, survival was not different among groups, and mortality was <20%. Lung weight/tibia length ratios were not significantly increased in MK-0626–treated mice (P = 0.09)

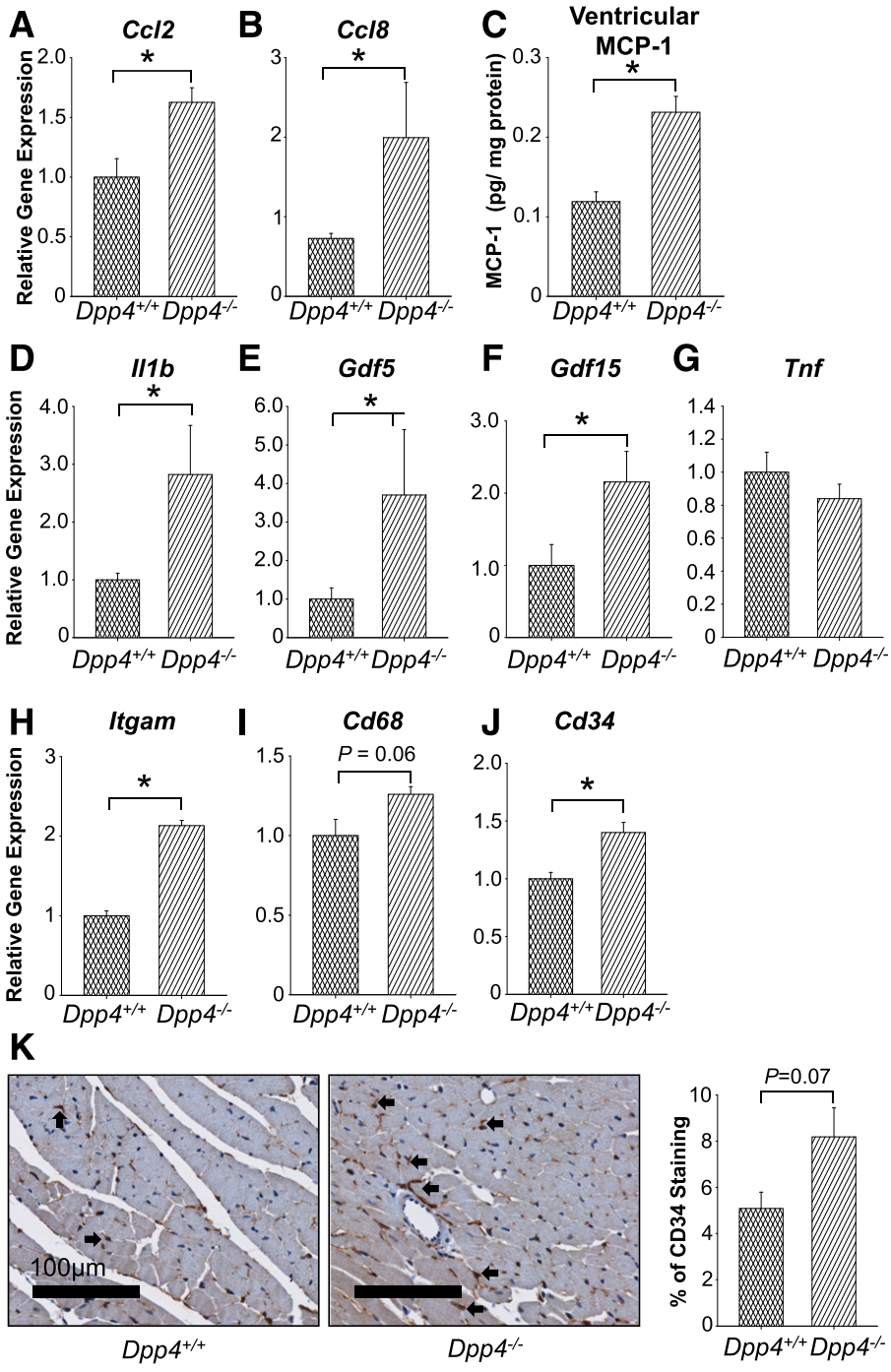

Figure 3—Markers of inflammation are elevated in euglycemic *Dpp4*$^{-/-}$ mice compared with littermate controls. Relative levels of ventricular mRNA of the inflammatory markers *Ccl2* (*A*) and *Ccl8* (*B*). *C*, Protein levels of ventricular MCP-1. Relative levels of ventricular mRNA of the inflammatory markers *Il1b* (*D*), *Gdf5* (*E*), *Gdf15* (*F*), *Tnf* (*G*), *Itgam* (*H*), *Cd68* (*I*), and *Cd34* (*J*). *K*, Representative images and quantitation of CD34 in sectioned hearts from *Dpp4*$^{-/-}$ mice compared with littermate controls (n = 4–5). Arrows represent areas of intense staining. All values are the mean ± SEM (n = 4–6, *P < 0.05).

(Fig. 4*C*). LVEF was significantly lower in MK-0626–treated mice but not in mice treated with liraglutide (Supplementary Table 4 and Fig. 4*D*). Gene expression analysis demonstrated a relatively greater increase in levels of cardiac *Nppa* mRNA transcripts in MK-0626–treated mice, whereas levels of *Nppb* were significantly elevated only in saline-treated mice after TAC surgery (Fig. 4*E* and *F*). No changes in mean tail-cuff blood pressure were observed among any of the groups (Fig. 4*G*). Mice treated with saline or liraglutide, but not MK-0626, demonstrated

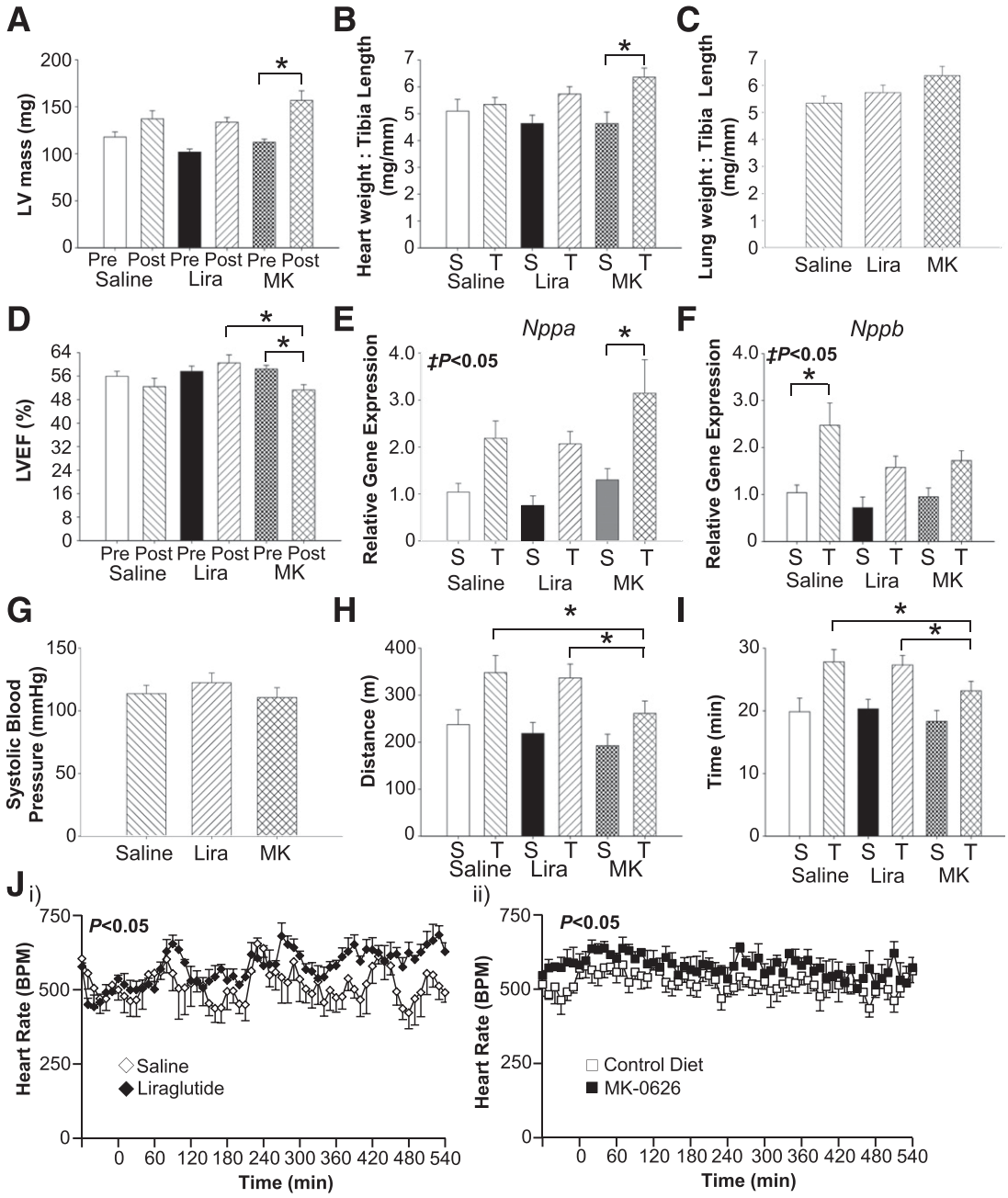

Figure 4—Older, dysglycemic C57BL/6J mice exhibit modest hypertrophy and decreased cardiac function in response to pressure overload–induced HF. Echocardiography was performed and tissues were harvested at 8 and 10 weeks post TAC surgery, respectively. *A*: LV mass, as determined by echocardiography. *B*, Heart weight/tibia length ratio. *C*, Lung weight/tibia length ratio (n = 5 sham-operated mice/group, n = 8–13 TAC mice/group). *D*: LVEF, as determined by echocardiography ($n \geq 10$/group). Relative levels of ventricular mRNA of the hypertrophic markers *Nppa* (*E*) and *Nppb* (*F*) (n = 5 sham-operated mice/group, n = 8–13 TAC mice/group). *G*, Systolic blood pressure as measured by CODA system tail cuff (N = 7–9/group). *H* and *I*, Distance and time run prior to exhaustion on a forced treadmill 8 weeks post TAC surgery. *J*, Heart rate measured by implanted telemetry devices (n = 4/group) i) in a separate group of mice injected with saline or liraglutide immediately prior to data collection or ii) in mice fed a control diet with or without MK-0626 for 24 h prior to data collection. Data presented are from the night cycle. All values are the mean ± SEM. *$P < 0.05$, ‡$P < 0.05$ sham surgery group (S) vs. TAC surgery group (T). Lira, liraglutide; MK, MK-0626; Post, post TAC surgery; Pre, pre-TAC surgery.

increased exercise tolerance, running for greater distances (and durations) prior to exhaustion (Fig. 4*H* and *I*). Consistent with previous findings (16), heart rate was elevated after liraglutide injection and was also higher in mice chronically treated with MK-0626 (Fig. 4*J*).

Markers of Fibrosis Are Elevated in Hearts From MK-0626–Treated Dysglycemic Mice

Surprisingly, levels of cardiac mRNA transcripts for collagen type I, alpha 1 (*Col1a1*); collagen type III, alpha 1 (*Col3a1*); and fibronectin (*Fn*) were elevated in hearts

from MK-0626–treated mice (Fig. 5*A–C*). Hearts from MK-0626–treated mice also demonstrated nonsignificant increases in trichrome staining and ventricular Col1a1 protein levels compared with saline-treated controls (Fig. 5*D* and *E*). α-Actin (*Acta2*) levels were elevated in all TAC surgery groups, whereas levels of gene products associated with collagen turnover, *Mmp2* and *Timp1*, were significantly increased in hearts from MK-0626–treated mice (Fig. 5*F–H*). *Mmp9* expression was reduced in all groups in response to TAC surgery (Supplementary Fig. 8*A*).

Inducers of Cardiac Fibrosis and Hypertrophy Are Elevated in Hearts From MK-0626–Treated Dysglycemic Mice

Key inducers of cardiac fibrosis, such as *Tgfb1*, *Tgfb2*, and angiotensinogen (*Agt*) (Fig. 6*A* and *B* and Supplementary Fig. 8*B*) were significantly increased in hearts from mice treated with MK-0626. Because TGF-β is secreted as a latent inactive complex, we also measured activated ventricular TGF-β1 protein, which trended higher in hearts from MK-0626–treated mice (Fig. 6*C*). No differences

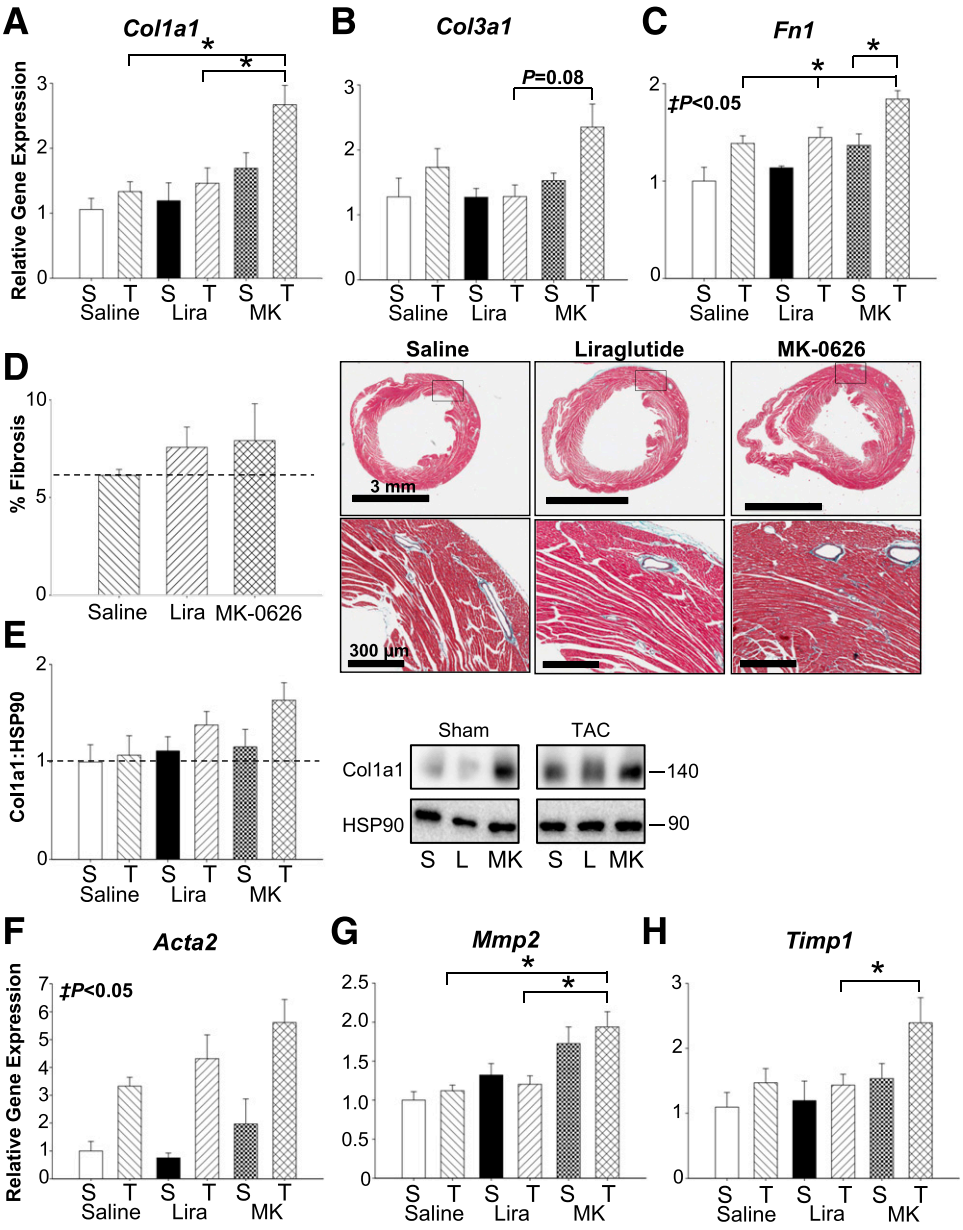

Figure 5—Markers of fibrosis are elevated in the hearts of MK-0626 (MK)–treated mice after surgical induction of pressure overload hypertrophy. Relative levels of ventricular mRNA of the fibrosis markers *Col1a1* (*A*), *Col3a1* (*B*), and *Fn1* (*C*). *D*, Representative images and quantification of Masson trichrome staining of hearts post TAC surgery (n = 3–4/group). Lower panels are magnifications of the boxed regions in the upper panels. *E*, Western blotting of Col1a1 normalized to Hsp90. L, liraglutide; S, saline. Relative levels of ventricular mRNA of the fibrosis markers *Acta2* (*F*), *Mmp2* (*G*), and *Timp1* (*H*). All values are the mean ± SEM (n = 5 sham surgery group [S], n = 8–13 TAC group [T]). *P < 0.05, ‡P < 0.05 sham surgery group vs. TAC surgery group. Lira, liraglutide.

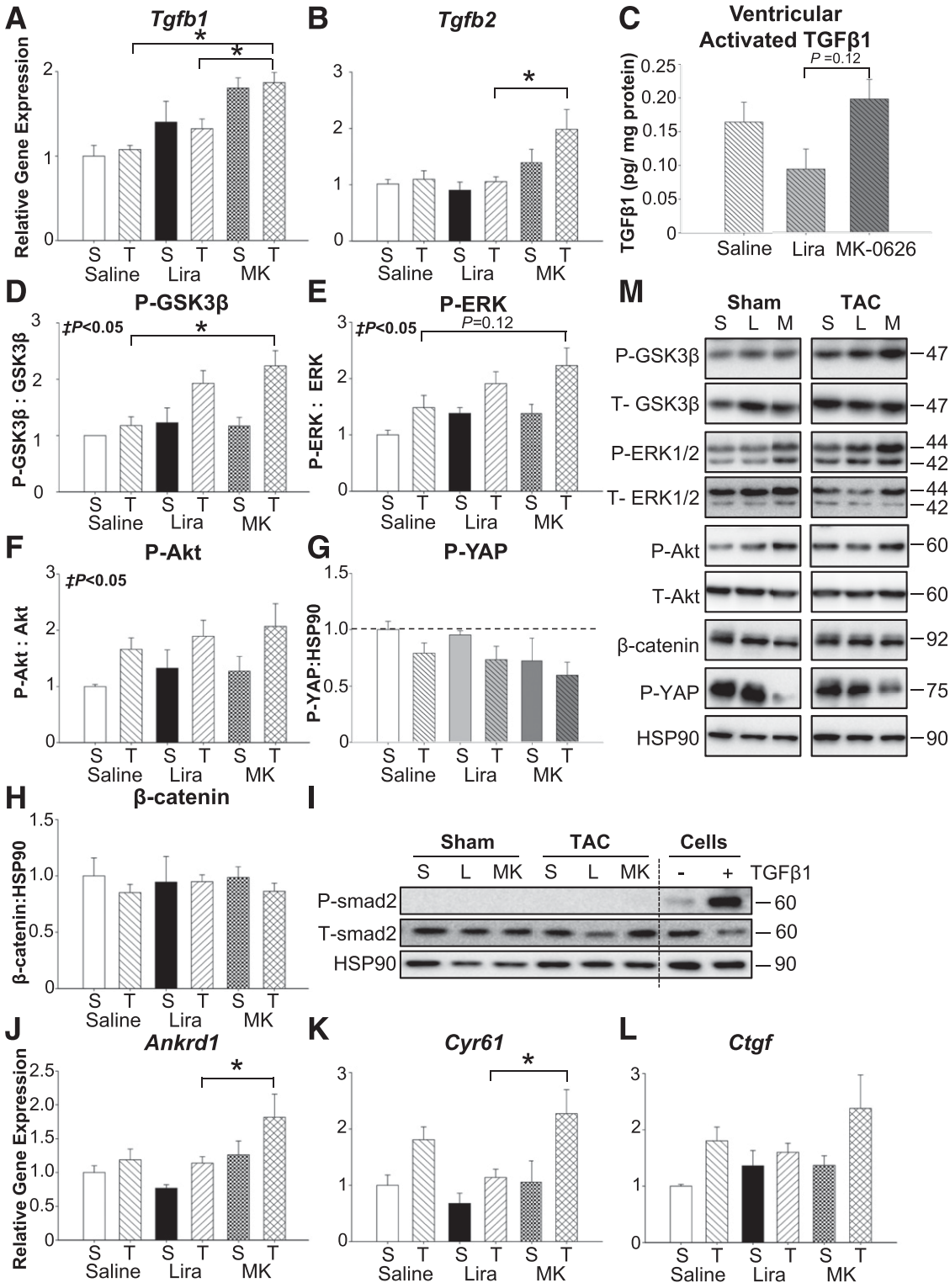

Figure 6—Inducers of fibrosis are elevated in the hearts of MK-0626 (MK)–treated mice after surgical induction of pressure overload hypertrophy. Relative levels of ventricular mRNA in the fibrosis markers *Tgfb1* (*A*) and *Tgfb2* (*B*). *C*, Activated ventricular TGF-β protein levels. Lysates were prepared from ventricular tissue (sham-operated or TAC mice treated with saline, liraglutide [Lira], or MK-0626). *D*, Phosphorylated (P) GSK-3β/GSK-3β ratio. *E*, Phosphorylated ERK/ERK ratio. *F*, Phosphorylated Akt/Akt ratio. *G*, Phosphorylated YAP/HSP90 ratio. *H*, β-Catenin/HSP90 ration. *I*, Phosphorylated Smad2/Smad2 ratio. Cellular positive control for antibodies was Eph4 mouse mammary epithelial cells treated with or without 100 pmol/L TGF-β for 1 h. L, liraglutide; S, saline. Relative levels of ventricular mRNA in the fibrosis and hypertrophy markers *Ankrd1* (*J*), *Cyr61* (*K*), and *Ctgf* (*L*). *M*, Representative blots for quantitations depicted in *D–H*. All values are the mean ± SEM (n = 3–5 for sham surgery group [S] and n = 8–13 for TAC [T]). *$P < 0.05$, ‡$P < 0.05$ sham surgery group vs. TAC surgery group.

were observed in cardiac expression of ACE 2 (*Ace2*), endothelin-1 (*Edn1*), and cardiotrophin-1 (*Ctf-1*) (Supplementary Fig. 8*C–E*). Hearts from MK-0626–treated mice exhibited increased cardiac levels of phosphorylated glycogen synthase kinase (GSK)-3β (Fig. 6*D* and *M*) and a nonsignificant increase in both phosphorylated ERK and Akt (Fig. 6*E*, *F*, and *M*).

As cardiac hypertrophy is associated with nuclear localization of Yes-associated protein (YAP), we assessed both the nuclear localization of YAP and the phosphorylation of YAP on residue Ser127, which results in cytosolic retention; changes in these parameters were not statistically significant between groups (Supplementary Fig. 9 and Fig. 6*G* and *M*). Other known TGF-β and Hippo signaling targets, including phosphorylation of small mother against decapentaplegic (Smad2) (Ser 465/467) and stabilization of β-catenin, were unchanged between groups (Fig. 6*H* and *M*). Conversely, the expression of some gene targets of these signaling pathways, specifically ankyrin repeat domain–containing protein 1 (*Ankrd1*), cysteine-rich angiogenic inducer (*Cyr61*), and connective tissue growth factor (*Ctgf*) were elevated in hearts from dysglycemic mice treated with MK-0626 compared with liraglutide (Fig. 6*J–L*).

Dysregulation of Inflammation-Related Cardiac Gene Expression Profiles in Hearts From MK-0626–Treated Mice

Intriguingly, *Tnf* was upregulated in hearts from MK-0626–treated diabetic mice (Fig. 7*A*), whereas both MK-0626 and liraglutide lowered cardiac *Il6* expression compared with saline-treated mice (Fig. 7*B*). In contrast with findings in $Dpp4^{-/-}$ mice, we did not observe differences in cardiac *Il1b*, *Ccl2*, *Ccl8*, and *Gdf15* expression (Supplementary Fig. 10*A–D*). We detected increased expression of the cardiac fibroblast collagen receptor *Ddr2*, but not *Vim* (Fig. 7*C* and Supplementary Fig. 10*E*), and increased levels of *Itgam* ($P = 0.12$), *Cd34*, and *Cd68* were also observed in cardiac RNA from MK-0626–treated mice (Fig. 7*D–F*). Furthermore, increased expression of *Hif1a*, *Nos3*, *Hmox1*, *Vegfa*, and *Nos2*, genes transducing the response to hypoxia, was evident in hearts after MK-0626 treatment (Supplementary Fig. 10*F–J*).

DISCUSSION

The unexpected report of increased hospitalization for HF in a clinical trial assessing the cardiovascular safety of saxagliptin (9) prompted us to assess the consequences of genetic *Dpp4* elimination or selective DPP4 inhibition in murine models of HF. Previous studies (12) demonstrated that $Dpp4^{-/-}$ mice exhibit a cardioprotective phenotype, encompassing improved survival and improved ventricular function, in response to coronary artery ligation or ischemia-reperfusion injury ex vivo. The current findings demonstrate that whole-body, germline disruption of the *Dpp4* gene in young, healthy, euglycemic mice attenuates the extent of adverse LV remodeling and preserves ventricular function after TAC-induced pressure overload HF or in response to doxorubicin administration. Whether the cardiovascular benefits attributable to genetic loss of DPP4 activity in preclinical studies are secondary to direct or indirect effects of reduced DPP4 activity and modulation of DPP4 substrate activity in the cardiovascular

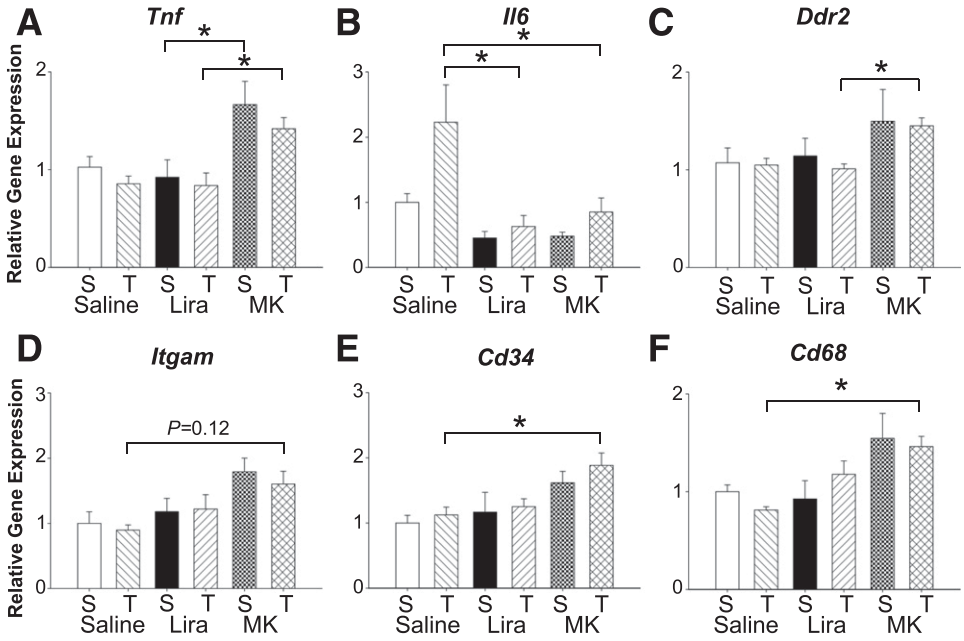

Figure 7—Levels of inflammatory markers are elevated in the hearts of dysglycemic C57BL/6J mice treated with MK-0626 (MK). Relative levels of ventricular mRNA of the inflammatory markers *Tnf* (*A*), *Il6* (*B*), *Ddr2* (*C*), *Itgam* (*D*), *Cd34* (*E*), and *Cd68* (*F*). All values are the mean ± SEM ($n = 5$ sham [S], $n = 8–13$ TAC [T] group). *$P < 0.05$. Lira, liraglutide.

system (6) or, alternatively, are influenced in part by the favorable metabolic phenotypes arising in *Dpp4*$^{-/-}$ mice (21,22) has not yet been ascertained.

In contrast to the cardioprotective phenotypes exhibited by euglycemic *Dpp4*$^{-/-}$ mice, prolonged treatment of older HFD-fed diabetic mice with MK-0626 and subjected to TAC did not improve cardiac function. Myocardial dysfunction and cardiomyocyte injury are commonly detected after the administration of STZ; however, whether this reflects the direct effects of STZ on the myocardium or arises independently from changes in the metabolic environment remains uncertain (23,24). MK-0626 is a highly selective orally available DPP4i (13) that produces sustained reduction of DPP4 activity in vivo. Our current findings were unexpected, as long-term therapy with MK-0626 in mice fed a HFD/high-fructose diet preserved cardiac structure and function, in association with decreased cardiac fibrosis (14). Notably, in a similar model, albeit with the added superimposed stress of TAC-induced HF, we observed the following: *1*) relative impairment of ventricular function, *2*) evidence for greater ventricular hypertrophy, and *3*) increased interstitial fibrosis in diabetic mice undergoing long-term treatment with MK-0626 post TAC surgery. Furthermore, mice treated with saline or liraglutide, but not MK-0626, exhibited increased functional exercise capacity (distance and time, Fig. 4*H* and *I*) after TAC through mechanisms that require further elucidation. The increase in cardiac hypertrophy in hearts from MK-0626–treated mice was accompanied by a significant induction of cardiac *Nppa* and an increase in the heart weight/tibia length ratio. In contrast, mice treated with liraglutide had no impairment of contractile function and no induction of fibrosis-related gene expression in response to pressure overload. Hence, the potentiation of GLP-1R signaling likely does not account for the adverse cardiovascular actions of MK-0626 in our studies.

The lack of improvement in ventricular function after treatment with a DPP4i in our current studies is not unique to experiments using MK-0626. Indeed, long-term administration of vildagliptin to normoglycemic rats both prior to and after the induction of myocardial infarction and HF did not attenuate the reduction of LVEF or modify cardiac remodeling (25). Similarly, the administration of saxagliptin to nondiabetic mice with HF secondary to cardiac-specific overexpression of Cre recombinase did not improve ventricular function or modify survival (26). Nevertheless, previous preclinical studies have not revealed a significant impairment of ventricular function after prolonged DPP4 inhibition.

Consistent with reduced interstitial fibrosis in hearts of MK-0626–treated C57BL/6J mice fed a HFD/high-fructose diet for 16 weeks (14), euglycemic *Dpp4*$^{-/-}$ mice also exhibited a significant reduction in cardiac fibrosis and no induction of fibrosis-related gene expression post TAC surgery. Considerable evidence also links the attenuation of DPP4 activity to improvement in ventricular function and reduced systemic and cardiac inflammation (6,27–29). Hence, we were surprised to detect increased cardiac expression of mRNA transcripts encoding multiple effectors of the immune response in normoglycemic mice with reduced DPP4 activity. Analysis of RNA from euglycemic *Dpp4*$^{-/-}$ mouse hearts revealed elevated levels of inflammation-related mRNA transcripts, including the macrophage chemokines *Ccl2*, *Ccl8*, and *Il-1b*, as well as members of the TGF-β chemokine family, *Gdf5* and *Gdf15*, but no differences in *Tnf* were observed. Furthermore, we observed increased levels of mRNAs corresponding to *1*) markers of cardiac fibroblasts, including *Ddr2* (30) and *Vim* (31), and *2*) infiltrating cells of bone marrow origin, such as *Cd34*, *Cd68*, and *Itgam*. Protein levels of MCP-1 and CD34 were also elevated in *Dpp4*$^{-/-}$ mice compared with littermate controls.

Although the precise mechanisms linking DPP4 inhibition to the development of cardiac fibrosis in our mouse model are incompletely understood, we hypothesize that the combination of hyperglycemia, an HFD, prolonged DPP4 inhibition in older mice, and the effects of pressure overload may combine to alter the milieu of growth factors, cytokines, and neurohumoral factors to promote a fibrogenic gene expression program. Although the clinical relevance of a single dose of STZ and 5 months of high-fat feeding in mice is questionable, diabetes is a significant risk for the development of organ fibrosis (32), and our model replicates the development of diabetes-associated cardiac fibrosis within a reasonable time frame.

Cardiac fibroblasts are responsible for the deposition of proteins encoded by *Col1a1*, *Col1a3*, and *Fn1* to maintain the integrity of the heart. All three gene products were elevated in diabetic MK-0626–treated mice, as was the cardiac fibroblast gene product *Ddr2*. Elevated levels of TGF-β are associated with both fibrosis and cardiac hypertrophy (33,34). We evaluated signaling through canonical and noncanonical mediators of fibrosis and hypertrophy in response to TGF-β, including ERK, GSK-3β/β-catenin (35), pSMAD2/SMAD2 (36), Akt (37), and YAP (38). Although we did not observe any robust changes in these effectors, these pathways are known to be activated in the short term in response to pressure overload and remain only moderately elevated at later time points (34,39). Therefore, in our assessment of hearts 12 weeks post TAC surgery, these pathways may not remain significantly perturbed. However, levels of direct transcriptional targets that have a known role in the progression of HF (*Col1a1*, *Col3a1*, *Fn1, Ankrd1*, *Cyr61*, and *Ctgf*) were all elevated, suggesting a role for TGF-β/Hippo pathway signaling in mediating the aberrant cardiac remodeling observed in mice treated with MK-0626.

Intriguingly, multiple DPP4 substrates increase cell proliferation and promote fibrosis, including neuropeptide Y, protein YY (40,41), and stromal-derived factor-1 (42). Furthermore, exposure to high glucose upregulates a transcriptional program enabling cardiac fibroblast proliferation, collagen synthesis, and cardiac fibrosis (43–45); upregulation of local angiotensin-II expression has also been linked to cardiac fibrosis (46). Moreover, high

glucose levels and increased levels of free fatty acids exert complementary effects to promote cardiomyocyte *Ctgf* expression, which in turn may independently promote cardiac fibrosis. The plausibility of DPP4 activity controlling the extent of cardiac fibrosis is further supported by data demonstrating that DPP4 inhibition potentiated the neuropeptide Y–dependent and protein YY–dependent regulation of cell proliferation and collagen synthesis in cardiac fibroblast cultures (41). Hence, we hypothesize that, under conditions characterized by sustained hyperglycemia, dyslipidemia, and pressure overload in older animals, reduction of DPP4 activity may further accelerate the development of cardiac fibrosis.

DPP4 is known to bind to the extracellular matrix and cleave collagen (47,48); however, the importance of DPP4 catalytic activity for collagen degradation has not been extensively studied in the heart. Although short-term systemic reduction of DPP4 activity altered the metabolism of circulating collagen-derived peptides in rats in vivo (49), whether DPP4 activity controls collagen metabolism in a heart subjected to metabolic stress and pressure overload has not been determined. Furthermore, DPP4, together with seprase, regulates fibroblast migration and invasion in the presence of a collagen matrix, with proteolytic activity of the DPP4-seprase complex modulating gelatin degradation and wound healing in a cell culture model ex vivo (50). We also detected reductions in cardiac *Mmp9* expression in mice after TAC surgery, and elevations in *Mmp2* and its inhibitor *Timp1* in hearts from MK-0626–treated mice that together may promote an imbalance in the degradation of extracellular matrix.

Our findings establish a preclinical model, encompassing long-term exposure to an HFD, experimental diabetes, and pressure overload–induced cardiac dysfunction, for understanding how the reduction of DPP4 activity may promote cardiac fibrosis and inflammation and impair ventricular function in older diabetic rodents. A major limitation of the current study is the use of only one DPP4i, MK-0626, in a single mouse model of cardiac dysfunction. Hence, our results cannot be generalized or extrapolated to other clinically used DPP4is. Our data provide an experimental preclinical model for further investigation of the pleiotropic cardiovascular mechanisms of actions of selective DPP4is in diabetic mice with impaired cardiac function.

Acknowledgments. The authors thank Dawei Qu and the Centre for Modeling Human Disease at the Lunenfeld-Tanenbaum Research Institute and Cindy Sawyez and the Metabolic Phenotyping Laboratory Core at the Robarts Research Institute for their excellent technical support. The authors also thank Dr. Masahiro Narimatsu and Dr. Jeff Wrana at the Lunenfeld-Tanenbaum Research Institute for helpful discussions.

Funding. This work was funded by the Heart and Stroke Foundation of Canada grant G-14-0005953. E.E.M. has received fellowship funding from the Canadian Diabetes Association and the Canadian Institutes of Health Research. J.R.U. was supported by fellowships from the Canadian Institutes of Health Research and the Alberta Innovates–Health Solutions. J.E.C. has received fellowships from the Banting & Best Diabetes Centre, the University of Toronto, and the Canadian Institutes of Health Research. D.J.D. is supported by a Canada Research Chair in Regulatory Peptides and a Banting & Best Diabetes Centre Novo Nordisk Chair in Incretin Biology.

Duality of Interest. J.R.U. has received a speaker's honorarium for symposia sponsored by Novo Nordisk. L.L.B. has served as a panel member and/or received a speaker's honorarium for symposia sponsored by Novo Nordisk, Merck Frosst, and GlaxoSmithKline LLC. D.J.D. has served as an advisor or consultant to Arisaph Pharmaceuticals, Intarcia, Merck Research Laboratories, MedImmune, Novo Nordisk, Receptos Inc., and Sanofi Inc. No other potential conflicts of interest relevant to this article were reported.

Author Contributions. E.E.M., E.M.V., J.R.U., J.E.C., and L.L.B. designed and carried out the experiments, analyzed the data, and wrote the article. K.W.A.B. and T.A. designed and carried out the experiments and analyzed the data. D.J.D. designed and analyzed the experiments and wrote the article. D.J.D. is the guarantor of this work and, as such, had full access to all the data in the study and takes responsibility for the integrity of the data and the accuracy of the data analysis.

References

1. Buse JB, Ginsberg HN, Bakris GL, et al.; American Heart Association; American Diabetes Association. Primary prevention of cardiovascular diseases in people with diabetes mellitus: a scientific statement from the American Heart Association and the American Diabetes Association. Diabetes Care 2007;30:162–172

2. Mazzone T, Chait A, Plutzky J. Cardiovascular disease risk in type 2 diabetes mellitus: insights from mechanistic studies. Lancet 2008;371:1800–1809

3. McMurray JJ, Gerstein HC, Holman RR, Pfeffer MA. Heart failure: a cardiovascular outcome in diabetes that can no longer be ignored. Lancet Diabetes Endocrinol 2014;2:843–851

4. Goldfine AB. Assessing the cardiovascular safety of diabetes therapies. N Engl J Med 2008;359:1092–1095

5. Campbell JE, Drucker DJ. Pharmacology, physiology, and mechanisms of incretin hormone action. Cell Metab 2013;17:819–837

6. Ussher JR, Drucker DJ. Cardiovascular actions of incretin-based therapies. Circ Res 2014;114:1788–1803

7. Zhong J, Maiseyeu A, Davis SN, Rajagopalan S. DPP4 in cardiometabolic disease: recent insights from the laboratory and clinical trials of DPP4 inhibition. Circ Res 2015;116:1491–1504

8. Green JB, Bethel MA, Armstrong PW, et al.; TECOS Study Group. Effect of sitagliptin on cardiovascular outcomes in type 2 diabetes. N Engl J Med 2015; 373:232–242

9. Scirica BM, Bhatt DL, Braunwald E, et al.; SAVOR-TIMI 53 Steering Committee and Investigators. Saxagliptin and cardiovascular outcomes in patients with type 2 diabetes mellitus. N Engl J Med 2013;369:1317–1326

10. White WB, Cannon CP, Heller SR, et al.; EXAMINE Investigators. Alogliptin after acute coronary syndrome in patients with type 2 diabetes. N Engl J Med 2013;369:1327–1335

11. Zannad F, Cannon CP, Cushman WC, et al.; EXAMINE Investigators. Heart failure and mortality outcomes in patients with type 2 diabetes taking alogliptin versus placebo in EXAMINE: a multicentre, randomised, double-blind trial. Lancet 2015;385:2067–2076

12. Sauvé M, Ban K, Momen MA, et al. Genetic deletion or pharmacological inhibition of dipeptidyl peptidase-4 improves cardiovascular outcomes after myocardial infarction in mice. Diabetes 2010;59:1063–1073

13. Edmondson SD, Mastracchio A, Mathvink RJ, et al. (2S,3S)-3-Amino-4-(3,3-difluoropyrrolidin-1-yl)-N,N-dimethyl-4-oxo-2-(4-[1,2,4]triazolo[1,5-a]-pyridin-6-ylphenyl)butanamide: a selective alpha-amino amide dipeptidyl peptidase IV inhibitor for the treatment of type 2 diabetes. J Med Chem 2006;49:3614–3627

14. Bostick B, Habibi J, Ma L, et al. Dipeptidyl peptidase inhibition prevents diastolic dysfunction and reduces myocardial fibrosis in a mouse model of Western diet induced obesity. Metabolism 2014;63:1000–1011

15. Noyan-Ashraf MH, Momen MA, Ban K, et al. GLP-1R agonist liraglutide activates cytoprotective pathways and improves outcomes after experimental myocardial infarction in mice. Diabetes 2009;58:975–983
16. Ussher JR, Baggio LL, Campbell JE, et al. Inactivation of the cardiomyocyte glucagon-like peptide-1 receptor (GLP-1R) unmasks cardiomyocyte-independent GLP-1R-mediated cardioprotection. Mol Metab 2014;3:507–517
17. Daugherty A, Rateri D, Hong L, Balakrishnan A. Measuring blood pressure in mice using volume pressure recording, a tail-cuff method. J Vis Exp 2009;(27): e1291
18. Massett MP, Berk BC. Strain-dependent differences in responses to exercise training in inbred and hybrid mice. Am J Physiol Regul Integr Comp Physiol 2005;288:R1006–R1013
19. Mulvihill EE, Assini JM, Sutherland BG, et al. Naringenin decreases progression of atherosclerosis by improving dyslipidemia in high-fat-fed low-density lipoprotein receptor-null mice. Arterioscler Thromb Vasc Biol 2010;30:742–748
20. Yusta B, Baggio LL, Koehler J, et al. GLP-1R agonists modulate enteric immune responses through the intestinal intraepithelial lymphocyte GLP-1R. Diabetes 2015;64:2537–2549
21. Marguet D, Baggio L, Kobayashi T, et al. Enhanced insulin secretion and improved glucose tolerance in mice lacking CD26. Proc Natl Acad Sci USA 2000; 97:6874–6879
22. Conarello SL, Li Z, Ronan J, et al. Mice lacking dipeptidyl peptidase IV are protected against obesity and insulin resistance. Proc Natl Acad Sci USA 2003; 100:6825–6830
23. Yu X, Tesiram YA, Towner RA, et al. Early myocardial dysfunction in streptozotocin-induced diabetic mice: a study using in vivo magnetic resonance imaging (MRI). Cardiovasc Diabetol 2007;6:6
24. Li Q, Li J, Ren J. UCF-101 mitigates streptozotocin-induced cardiomyocyte dysfunction: role of AMPK. Am J Physiol Endocrinol Metab 2009;297:E965–E973
25. Yin M, Silljé HH, Meissner M, van Gilst WH, de Boer RA. Early and late effects of the DPP-4 inhibitor vildagliptin in a rat model of post-myocardial infarction heart failure. Cardiovasc Diabetol 2011;10:85
26. Vyas AK, Aerni-Flessner LB, Payne MA, Kovacs A, Jay PY, Hruz PW. Saxagliptin improves glucose tolerance but not survival in a murine model of dilated cardiomyopathy. Cardiovasc Endocrinol 2012;1:74–82
27. Miyoshi T, Nakamura K, Yoshida M, et al. Effect of vildagliptin, a dipeptidyl peptidase 4 inhibitor, on cardiac hypertrophy induced by chronic beta-adrenergic stimulation in rats. Cardiovasc Diabetol 2014;13:43
28. Liu YS, Huang ZW, Wang L, et al. Sitagliptin alleviated myocardial remodeling of the left ventricle and improved cardiac diastolic dysfunction in diabetic rats. J Pharmacol Sci 2015;127:260–274
29. Mulvihill EE, Drucker DJ. Pharmacology, physiology, and mechanisms of action of dipeptidyl peptidase-4 inhibitors. Endocr Rev 2014;35:992–1019
30. Cowling RT, Yeo SJ, Kim IJ, et al. Discoidin domain receptor 2 germline gene deletion leads to altered heart structure and function in the mouse. Am J Physiol Heart Circ Physiol 2014;307:H773–H781
31. Bei Y, Zhou Q, Fu S, et al. Cardiac telocytes and fibroblasts in primary culture: different morphologies and immunophenotypes. PLoS One 2015;10: e0115991
32. Asbun J, Villarreal FJ. The pathogenesis of myocardial fibrosis in the setting of diabetic cardiomyopathy. J Am Coll Cardiol 2006;47:693–700
33. Takahashi N, Calderone A, Izzo NJ Jr, Mäki TM, Marsh JD, Colucci WS. Hypertrophic stimuli induce transforming growth factor-beta 1 expression in rat ventricular myocytes. J Clin Invest 1994;94:1470–1476
34. Kuwahara F, Kai H, Tokuda K, et al. Transforming growth factor-beta function blocking prevents myocardial fibrosis and diastolic dysfunction in pressure-overloaded rats. Circulation 2002;106:130–135
35. Caraci F, Gili E, Calafiore M, et al. TGF-beta1 targets the GSK-3beta/beta-catenin pathway via ERK activation in the transition of human lung fibroblasts into myofibroblasts. Pharmacol Res 2008;57:274–282
36. Euler-Taimor G, Heger J. The complex pattern of SMAD signaling in the cardiovascular system. Cardiovasc Res 2006;69:15–25
37. Xin M, Kim Y, Sutherland LB, et al. Hippo pathway effector Yap promotes cardiac regeneration. Proc Natl Acad Sci USA 2013;110:13839–13844
38. Varelas X. The Hippo pathway effectors TAZ and YAP in development, homeostasis and disease. Development 2014;141:1614–1626
39. Villarreal FJ, Dillmann WH. Cardiac hypertrophy-induced changes in mRNA levels for TGF-beta 1, fibronectin, and collagen. Am J Physiol 1992;262:H1861–H1866
40. Cheng D, Zhu X, Gillespie DG, Jackson EK. Role of RACK1 in the differential proliferative effects of neuropeptide Y(1-36) and peptide YY(1-36) in SHR vs. WKY preglomerular vascular smooth muscle cells. Am J Physiol Renal Physiol 2013; 304:F770–F780
41. Zhu X, Gillespie DG, Jackson EK. NPY1-36 and PYY1-36 activate cardiac fibroblasts: an effect enhanced by genetic hypertension and inhibition of dipeptidyl peptidase 4. Am J Physiol Heart Circ Physiol 2015;309:H1528–H1542
42. Chu PY, Zatta A, Kiriazis H, et al. CXCR4 antagonism attenuates the cardiorenal consequences of mineralocorticoid excess. Circ Heart Fail 2011;4:651–658
43. Shamhart PE, Luther DJ, Adapala RK, et al. Hyperglycemia enhances function and differentiation of adult rat cardiac fibroblasts. Can J Physiol Pharmacol 2014;92:598–604
44. Bugyei-Twum A, Advani A, Advani SL, et al. High glucose induces Smad activation via the transcriptional coregulator p300 and contributes to cardiac fibrosis and hypertrophy. Cardiovasc Diabetol 2014;13:89
45. Aguilar H, Fricovsky E, Ihm S, et al. Role for high-glucose-induced protein O-GlcNAcylation in stimulating cardiac fibroblast collagen synthesis. Am J Physiol Cell Physiol 2014;306:C794–C804
46. Singh VP, Le B, Khode R, Baker KM, Kumar R. Intracellular angiotensin II production in diabetic rats is correlated with cardiomyocyte apoptosis, oxidative stress, and cardiac fibrosis. Diabetes 2008;57:3297–3306
47. Löster K, Zeilinger K, Schuppan D, Reutter W. The cysteine-rich region of dipeptidyl peptidase IV (CD 26) is the collagen-binding site. Biochem Biophys Res Commun 1995;217:341–348
48. Bermpohl F, Löster K, Reutter W, Baum O. Rat dipeptidyl peptidase IV (DPP IV) exhibits endopeptidase activity with specificity for denatured fibrillar collagens. FEBS Lett 1998;428:152–156
49. Jost MM, Lamerz J, Tammen H, et al. In vivo profiling of DPP4 inhibitors reveals alterations in collagen metabolism and accumulation of an amyloid peptide in rat plasma. Biochem Pharmacol 2009;77:228–237
50. Ghersi G, Dong H, Goldstein LA, et al. Regulation of fibroblast migration on collagenous matrix by a cell surface peptidase complex. J Biol Chem 2002;277: 29231–29241

SUPPLEMENTARY DATA

Supplementary Table I. List of antibodies with manufacturers reference number

Antibody	Reference	Company	Application
Anti-Akt	9272	Cell Signaling Technologies	Western-blot
Anti-collagen 1 [COL-1]	ab90395	Abcam	Western-blot
Anti-CD34	ab8158	Abcam	Immunostaining
Anti-ERK	9102	Cell Signalling Technologies	Western-blot
Anti-GSK3β	9315	Cell Signaling Technologies	Western-blot
Anti-hsp90	610418	BD Biosciences	Western-blot
Anti-phospho ERK1/2 (Thr 202/Tyr204)	9101	Cell Signaling Technologies	Western-blot
Anti-phospho Smad2 (Ser465/467)	3101/3108	Cell Signaling Technologies	Western-blot
Anti-phospho YAP (Ser127)	4911	Cell Signaling Technologies	Western-blot
Anti-phospho-Akt (Ser 473)	9271	Cell Signaling Technologies	Western-blot
Anti-phospho-GSK3β (Ser 9)	9331	Cell Signaling Technologies	Western-blot
Anti-Smad2	5339	Cell Signaling Technologies	Western-blot
Anti-YAP	14074	Cell Signaling Technologies	Immunostaining
Anti-β-catenin	BD610153	BD Biosciences	Western-blot

SUPPLEMENTARY DATA

Supplementary Table II. List of primers and probes used with Life Technology inventory number

Gene symbol	Gene name	Mouse primer
Ace2	angiotensin I converting enzyme 2	Mm01159003_m1
Acta1	actin, alpha 1, skeletal muscle	Mm00808218_g1
Acta2	actin, alpha 2, smooth muscle, aorta	Mm01546133_m1
Agtr1	angiotensin II receptor, type I	Mm00507771_m1
Agt	angiotensinogen	Mm00657574_s1
Ankrd1	ankyrin repeat domain containing protein 1	Mm00496512_m1
Ccl2	chemokine (C-C motif) ligand 2 (MCP-1)	Mm00441242_m1
Ccl8	chemokine (C-C motif) ligand 8 (MCP-2)	Mm01297183_m1
Cd34	CD34 antigen	Mm00519283_m1
Cd68	CD68 antigen	Mm00839636_g1
Col1a1	collagen type1α1	Mm01254476_m1
Col3a1	collagen type 3α1	Mm00801666_g1
Ctf1	cardiotrophin-1	Mm00432772_m1
Ctgf	connective tissue growth factor	Mm01192932_g1
Cyr61	cysteine-rich angiogenic inducer	Mm00487498_m1
Ddr2	discoidin domain receptor family, member 2	Mm00445615_m1
Edn1	endothelin 1	Mm00438656_m1
Fn1	fibronectin-1	Mm01256744_m1
Gdf15	growth differentiation factor 15	Mm00442228_m1
Gdf5	growth differentiation factor 5	Mm00433564_m1
Hif1a	hypoxia inducible factor 1, alpha subunit	Mm00468869_m1
Hmox1	heme oxygenase (decycling) 1	Mm00516005_m1
Il1b	interleukin 1 beta	Mm01336189_m1
Il6	interleukin 6	Mm00446190_m1
Itgam	integrin alpha M (CD11b)	Mm00434455_m1
Mmp2	matrix metallopeptidase 2	Mm00439498_m1
Mmp9	matrix metallopeptidase 9	Mm00442991_m1
Nos2	nitric oxide synthase 2, inducible	Mm00440485_m1
Nos3	nitric oxide synthase 3, endothelial cell	Mm00435204_m1
Nppa	natriuretic peptide type A	Mm01255748_g1
Nppb	natriuretic peptide type B	Mm01255770_g1
Ppia	peptidylprolyl isomerase A	Mm02342430_g1
Tgfb1	transforming growth factor, beta 1	Mm01178820_m1
Tgfb2	transforming growth factor, beta 2	Mm00436955_m1
Timp1	tissue inhibitor of metalloproteinase 1	Mm00441818_m1
Tnf	tumor necrosis factor α	Mm00443258_m1
Vegfa	vascular endothelial growth factor A	Mm01281449_m1
Vim	vimentin	Mm01333430_m1

SUPPLEMENTARY DATA

Supplementary Figure I. Genetic disruption of the *Dpp4* gene improves glucose tolerance, reduces Dpp4 activity and elevates GLP-1 levels but does not disrupt basal cardiac structure and function. Mice were fasted 6 hours prior to glucose tolerance test and measurement of plasma parameters. **A-B:** Oral glucose tolerance was significantly improved by genetic deletion of *Dpp4*. **C:** Fasting plasma active GLP-1 levels are elevated (n≥5/group). **D:** DPP4 activity was significantly reduced in *Dpp4-/-* mice as determined by fluorometric assay (n≥5/group). **E**. Fasting blood glucose was not changed between genotypes. **F & G:** Body weight and MRI analysis of body fat was performed at 12 weeks of age (n≥8/group). **H-K:** Baseline cardiac parameters determined by echocardiography are not changed in *Dpp4-/-* mice compared with wild-type controls (n≥8/group). All values are mean±SEM **P*<0.05.

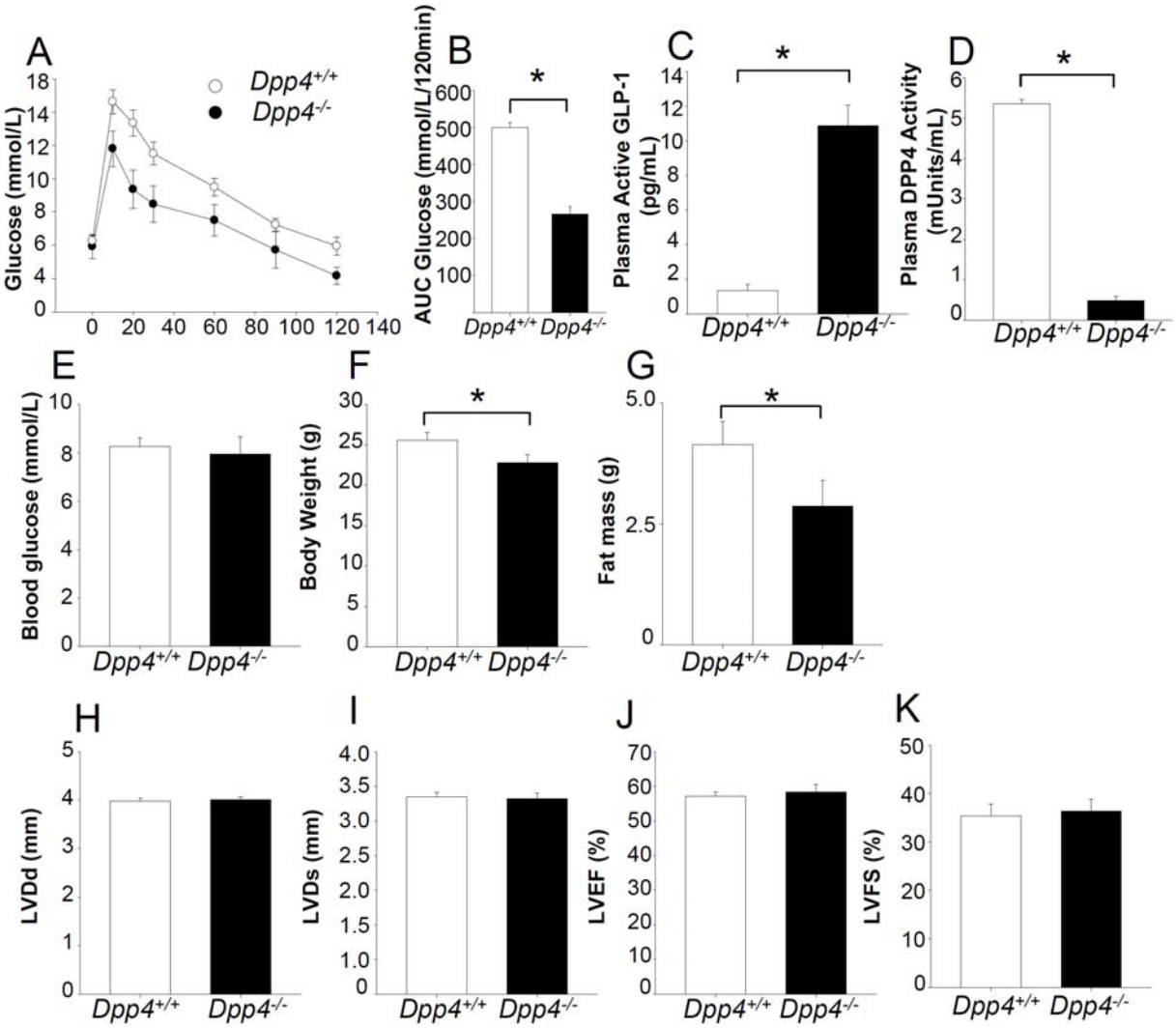

SUPPLEMENTARY DATA

Supplementary Figure II.

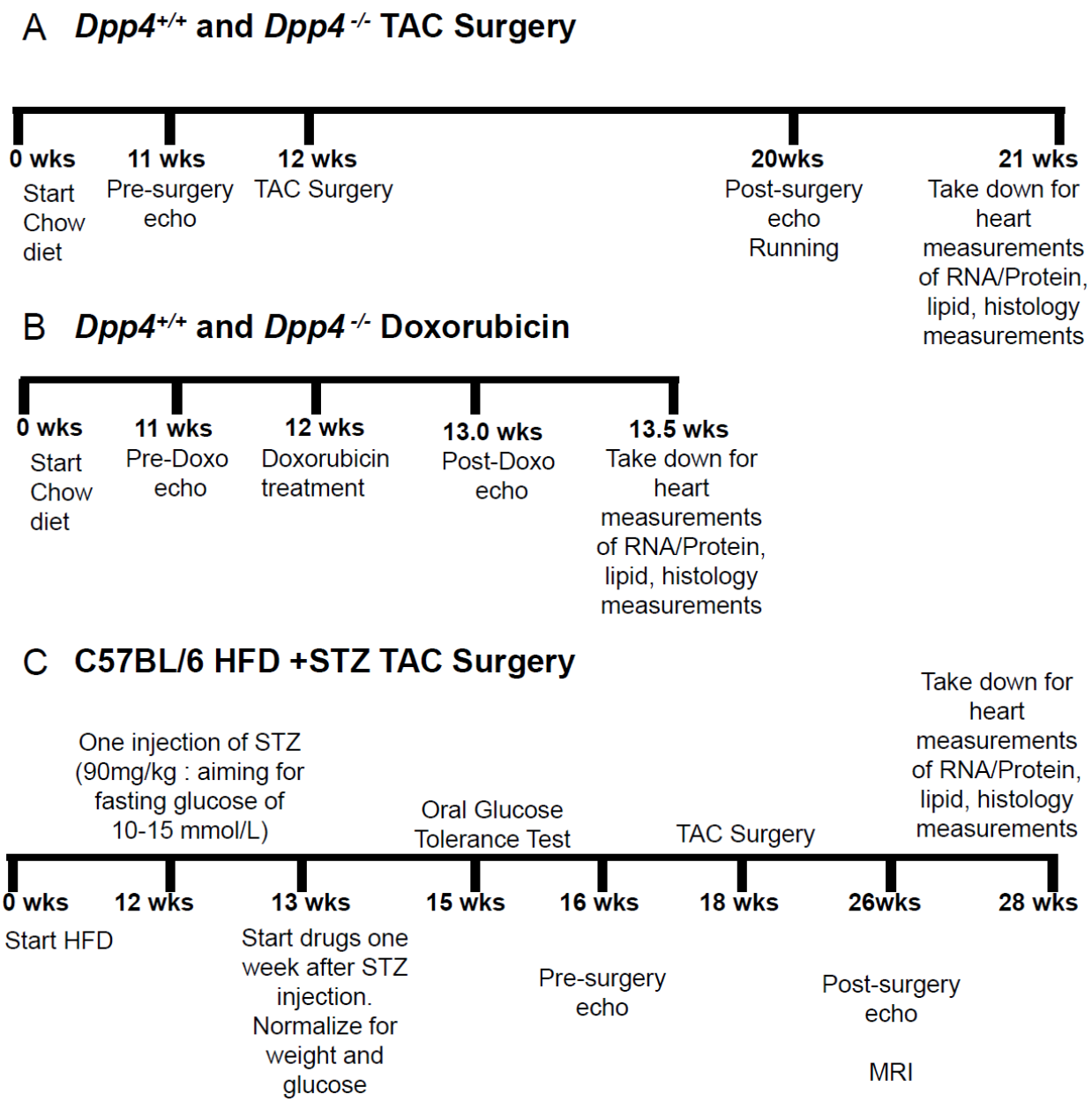

SUPPLEMENTARY DATA

Supplementary Table III. Echocardiography-defined dimensional and functional parameters in young, euglycemic *Dpp4*+/+ and *Dpp4*-/- littermates preoperatively or post TAC- surgery

	Dpp4$^{+/+}$			*Dpp4*$^{-/-}$		
	Pre TAC	Post TAC		Pre TAC	Post TAC	
IVS;d	0.89 ± 0.05	1.34 ± 0.09	*	0.85 ± 0.06	1.10 ± 0.12	*
IVS;s	1.28 ± 0.11	1.74 ± 0.12	*	1.37 ± 0.12	1.60 ± 0.07	*
Diameter;s	3.16 ± 0.12	4.75 ± 0.34	* ¶	2.80 ± 0.18	3.45 ± 0.15	*
Diameter;d	4.26 ± 0.10	5.42 ± 0.29	*	4.08 ± 0.18	4.57 ± 0.09	*
Volume;s	39.90 ± 3.64	86.10 ± 14.31	* ¶	30.20 ± 4.84	49.47 ± 5.44	*
Volume;d	81.21 ± 4.49	121.93 ± 13.98	* ¶	73.86 ± 7.98	95.96 ± 4.56	*
Stroke Volume	41.31 ± 3.70	35.63 ± 3.40		43.66 ± 3.42	46.49 ± 3.25	
Ejection Fraction	50.86 ± 3.62	27.26 ± 3.14	* ¶	59.70 ± 2.54	48.72 ± 3.74	*
Fractional Shortening	25.70 ± 2.28	12.98 ± 1.67	* ¶	31.42 ± 1.72	24.62 ± 2.28	*
Cardiac Output	19.34 ± 3.48	19.55 ± 1.88		19.89 ± 1.50	24.93 ± 3.10	
LV Mass	119.52 ± 27.24	264.70 ± 18.24	*	92.93 ± 3.14	194.6 ± 14.93	*
LVID;d	4.25 ± 0.22	5.01 ± 0.26	*	4.16 ± 0.21	4.58 ± 0.12	*
LVID;s	3.12 ± 0.15	4.36 ± 0.34	* ¶	2.77 ± 0.23	3.47 ± 0.12	*
LVPW;d	0.78 ± 0.05	1.22 ± 0.04	*	0.74 ± 0.04	1.14 ± 0.16	*
LVPW;s	1.18 ± 0.10	1.44 ± 0.05	*	1.19 ± 0.05	1.53 ± 0.14	*

All values are mean±SEM
* $P<0.05$ compared with Pre-TAC surgery
¶ $P<0.05$ compared with *Dpp4*-/- mice

SUPPLEMENTARY DATA

Supplementary Figure III. Genetic disruption of the Dpp4 gene improves cardiovascular outcomes following doxorubicin induced cardiomyopathy. Dpp4-/- mice or Dpp4+/+ littermate controls were evaluated prior to or 10 days post doxorubicin injection A: Body weight change observed after doxorubicin treatment (n≥6/group). B: Heart weight normalized to tibia length (n≥6/group). Cardiac Echocardiography parameters C: LV mass, D: LVDs, E: LVDd (n≥6/group). Relative levels of ventricular mRNA of the hypertrophic markers F: Nppa (Anp) and G: Nppb (Bnp) normalized to Ppia. (n≥6/group). All values are mean±SEM *P<0.05, †P<0.05 sham surgery group vs. doxorubicin treated group.

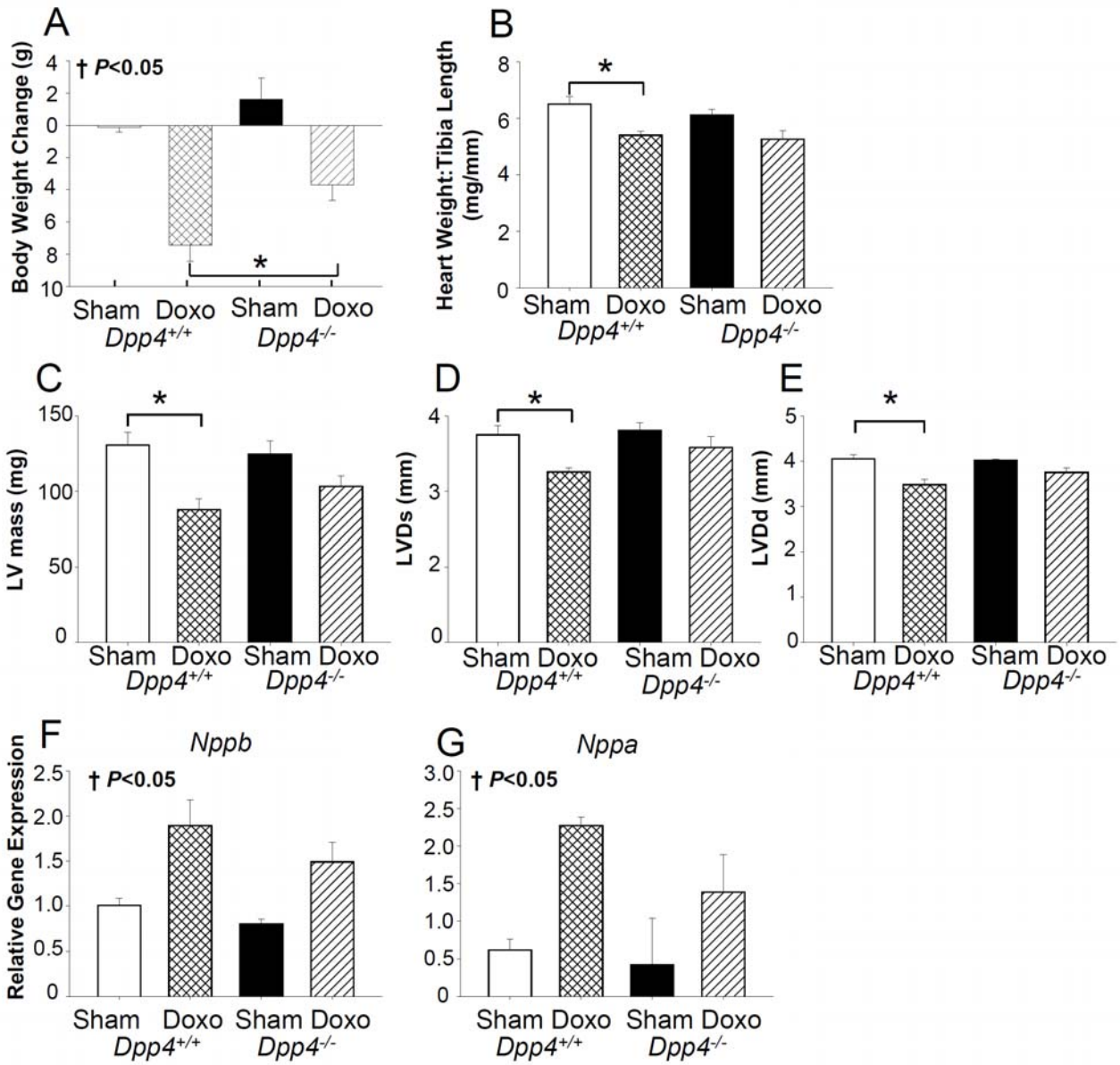

SUPPLEMENTARY DATA

Supplementary Figure IV. Genetic disruption of the *Dpp4* gene improves fibrosis following doxorubicin-induced cardiomyopathy. *Dpp4-/-* mice or *Dpp4+/+* littermate controls were evaluated 10 days post doxorubicin injection. Relative levels of ventricular mRNA of the fibrosis markers **A:** *TgfB2*, **B:** *Mmp9* **C:** *Timp1,* **and D:** *Col1a1* normalized to *Ppia* (n≥8/group). Western blot analysis was performed using lysates prepared from ventricular tissue from sham or doxorubicin treated *Dpp4-/-* mice or *Dpp4+/+* littermate controls. **E:** Phospho-ERK (phospho-Thr202/Tyr 204) normalized to total ERK. **F:** Phospho-Akt (Phospho-473) normalized to total Akt. (n≥5/group). All values are mean±SEM **P*<0.05, †*P*<0.05 sham surgery group vs. TAC surgery group.

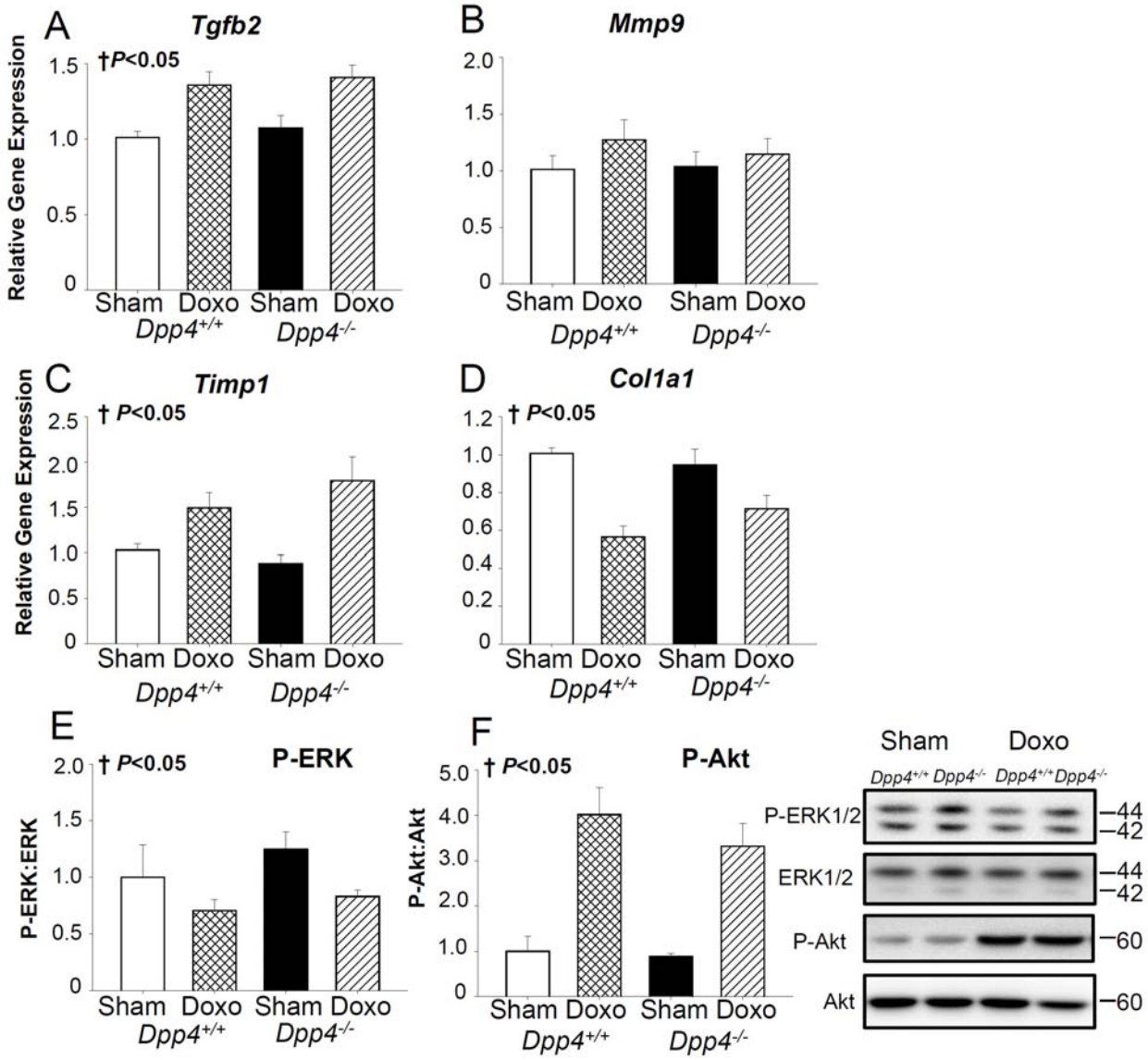

SUPPLEMENTARY DATA

Supplementary Figure V. Genetic disruption of the *Dpp4* gene had no effect on markers of hypoxia and revascularization. Relative expression levels of ventricular mRNA of the hypoxia and revascularization markers **A:** *Hmox1*, **B:** *Nos2*, **C:** *Nos3*, **D:** *Hif1a*, **E:** *Vegfa*, **F:***Il6* (n =4- 5/group). All values are mean±SEM **P*<0.05.

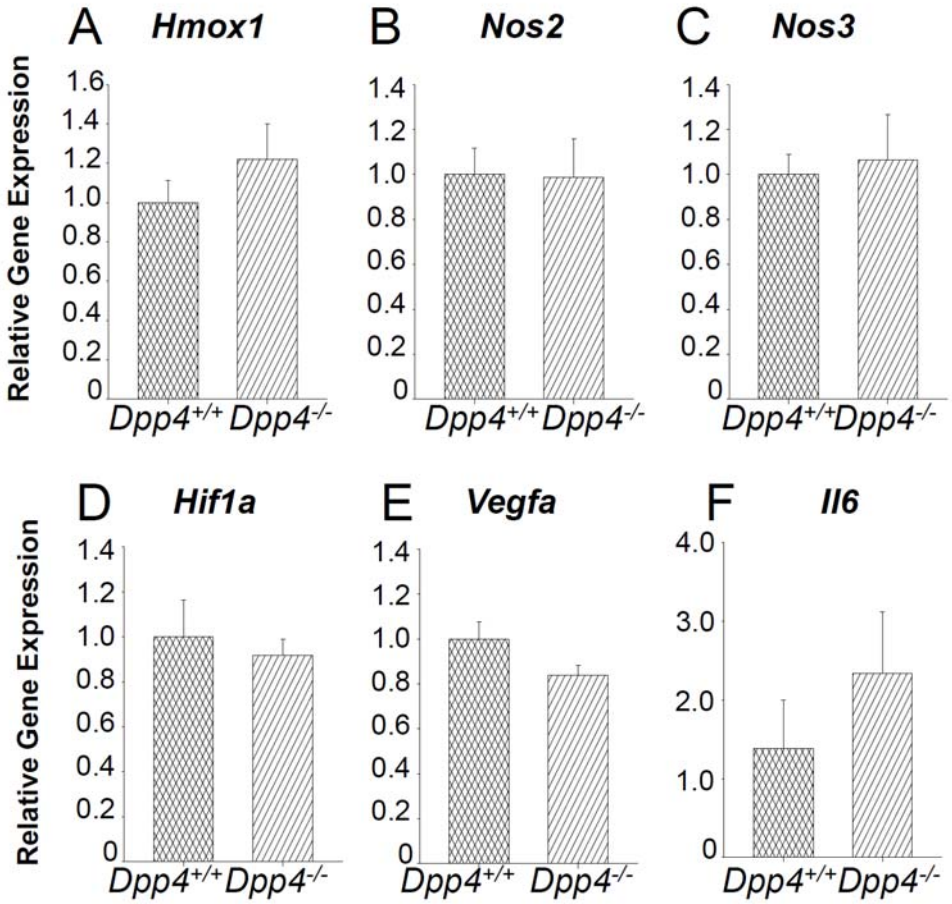

SUPPLEMENTARY DATA

Supplementary Figure VI. The glucose lowering effects of MK-0626 are dependent on DPP4. *Dpp4*+/+ and *Dpp4*-/- mice were fasted for 6 hours, then gavaged with water or 3mg/kg of MK-0626 (n=8 for *Dpp4*+/+, n=6-7 for *Dpp4*-/-) 30min prior to glucose oral gavage of 2g/kg body weight. **A:** Glucose excursions for *Dpp4*+/+ +/- MK-0626, **B:** Glucose excursions for *Dpp4*-/- +/- MK-0626. **C:** Corresponding AUC and **D:** Dpp4 activity are presented during the oGTT. All values are means +/- SEM. **P*<0.05

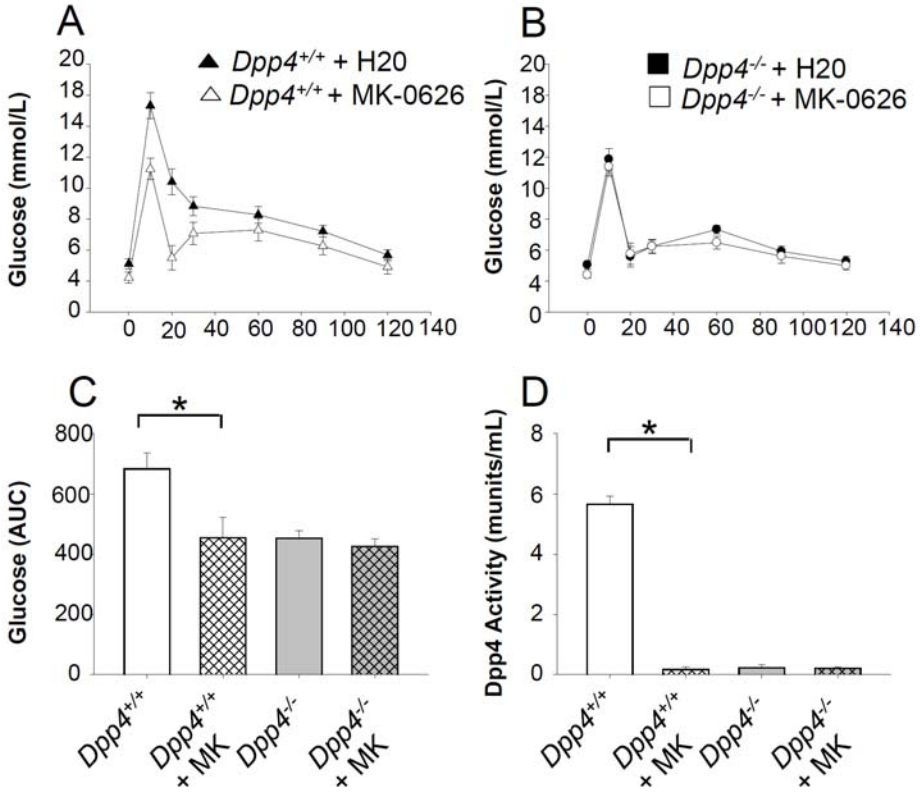

SUPPLEMENTARY DATA

Supplementary Figure VII. Both liraglutide and MK-0626 improve metabolic parameters in high fat fed, diabetic C57BL/6J mice. A: Oral glucose tolerance following an overnight fast after two weeks of pharmacological treatment but prior to TAC surgery (n≥10/group), **B:** Four hour fasting HbA1c in NGSP % (IFCC units Saline = 43mmol/mol, Liraglutide = 30mmol/mol, MK626 = 32mmol/mol) **C:** Glucose in mice 10 weeks after TAC surgery (n≥8/group), **D:** Fasting plasma insulin and levels at 10 minutes post-glucose during the GTT in **A** (n≥10/group). **E:** Dpp4 activity following a 4 hour fast in mice 10 weeks after TAC surgery (n≥8/group). **F:** Plasma active GLP-1 levels after 16 hours of fasting and at 10 minutes post-glucose during the GTT in **A** (n≥10/group). Four hour fasting plasma **G:** Triglycerides and **H:** Cholesterol in mice 10 weeks after TAC surgery (n≥5/group). **I:** Body weight was elevated in mice treated with MK-0626 which was related to increased food intake **J** (n≥10/group). **K/L:** MRI analysis indicate that the increased body weight in MK-0626- treated mice was associated with an accumulation of fat mass but no change in lean mass was observed (n≥10/group). All values are mean±SEM **P*<0.05.

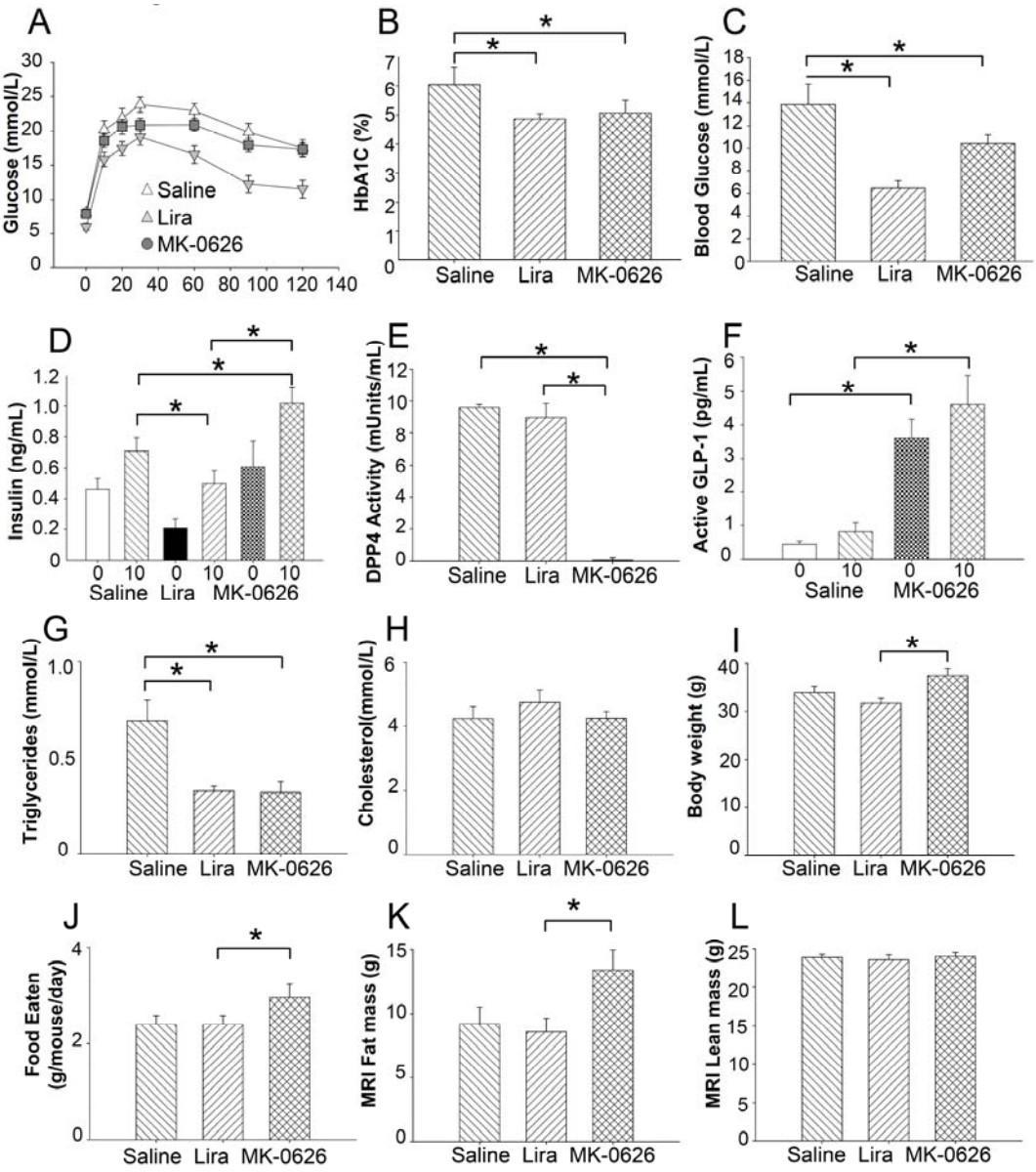

SUPPLEMENTARY DATA

Supplementary Table IV. Echocardiography-defined dimensional and functional parameters in older, dysglycemic C57BL/6J mice treated with saline, liraglutide or the DPP4 inhibitor MK-0626, preoperatively or post TAC-surgery.

		Saline		Liraglutide		MK-0626	
C57BL/6J		Pre-TAC surgery	Post-TAC surgery	Pre-TAC surgery	Post-TAC surgery	Pre-TAC surgery	Post-TAC surgery
IVS;d	mm	1.11 ± 0.04	1.15±0.10	1.00±0.05	1.18±0.05	1.05±0.03	1.15±0.06
IVS;s	mm	1.55 ± 0.06	1.54±0.11	1.41±0.05	1.67±0.07	1.48±0.04	1.60±0.09
Diameter;s	mm	2.87 ± 0.07	2.90±0.24	2.79±0.08	2.75±0.23	2.81±0.08	3.00±0.19
Diameter;d	mm	4.03 ± 0.05	4.05±0.22	4.00±0.05	4.05±0.16	4.05±0.07	4.18±0.19
Volume;s	µL	31.89 ± 1.77	32.95±3.32	30.02±2.33	28.29±2.50	30.50±1.98	35.89±2.87
Volume;d	µL	71.67 ± 1.91	72.46±2.18	70.26±2.06	72.47±3.16	72.39±2.82	78.19±3.40
Stroke Volume	µL	39.78 ± 1.12	39.52±2.85	40.23±1.61	43.13±2.00	41.89±1.32	42.26±2.19
Ejection Fraction	%	55.97 ± 1.68	52.43±3.19	57.61±2.25	60.52±2.74	58.39±1.52	51.73±1.71*
Fractional Shortening	%	29.06 ± 1.14	26.14±1.82	30.16±1.46	32.32±1.85	30.62±1.07	26.85±1.00 *
Cardiac Output	mL/min	18.31 ± 0.63	19.54±1.67	18.76±0.73	21.40±1.00	18.89±0.79	20.30±1.02
LV Mass	mg	117.8 ± 5.37	130.76±11.2	101.80±2.96	133.45±5.23	112.18±2.61	156.76±11.77*
LVID;d	mm	3.24 ± 0.34	4.01±0.07	2.93±0.41	3.96±0.09	3.22±0.32	4.12±0.09
LVID;s	mm	3.14 ± 0.14	3.05±0.10	3.20±0.17	2.68±0.13	3.17±0.14	3.04±0.10
LVPW;d	mm	0.89 ± 0.02	0.91±0.09	0.82±0.02	0.95±0.05	0.83±0.01	1.17±0.09
LVPW;s	mm	1.24 ± 0.03	1.26±0.06	1.16±0.05	1.40±0.05	1.23±0.04	1.48±0.04

All values are mean±SEM (n≥8) * *P*<0.05 compared with pre-TAC

SUPPLEMENTARY DATA

Supplementary Figure VIII. Markers of ECM remodeling and fibrosis are increased or unchanged in MK-0626-treated high fat fed, diabetic C57BL/6J mice after surgical induction of pressure overload. Relative change of ventricular mRNA levels of **A:** *Mmp9*, **B:** *Agt*, **C:** *Ace2*, **D:** *Edn-1*, **E:** *Ctf-1* (n≥5 sham group (S) and n=8-13 TAC group (T)). All values are mean±SEM **P*<0.05.

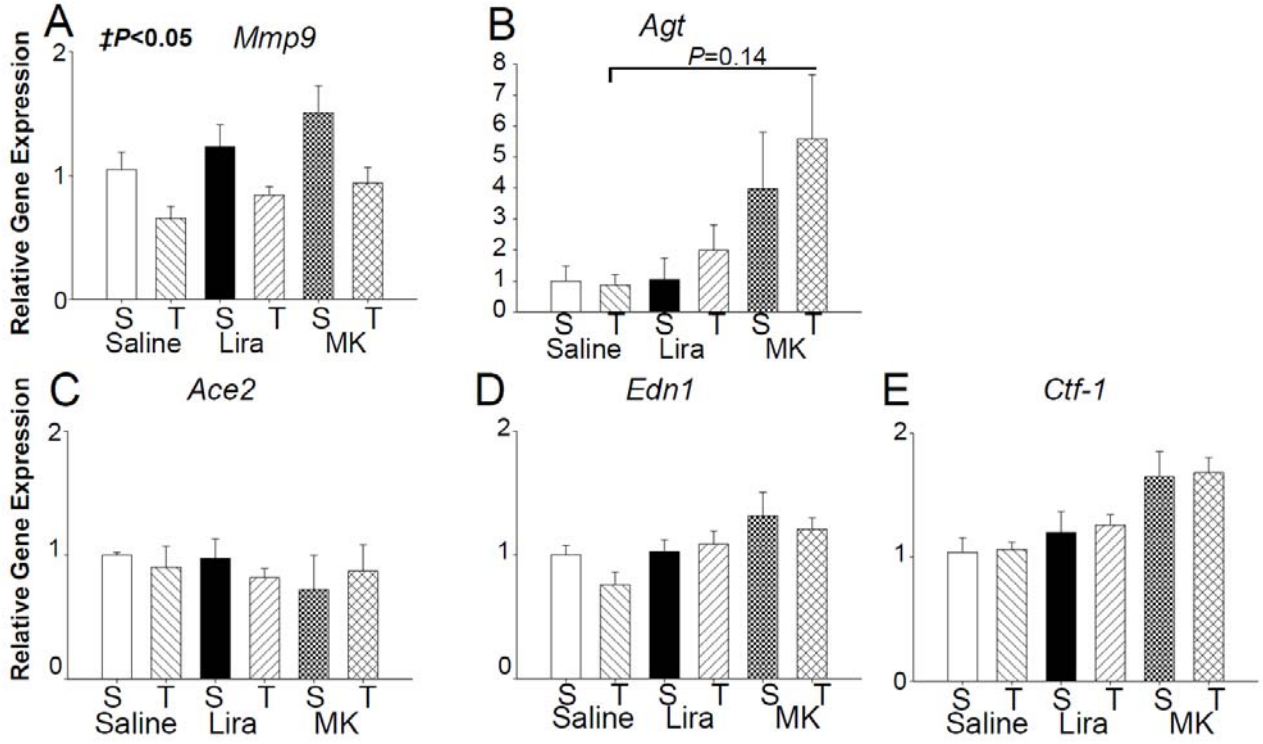

SUPPLEMENTARY DATA

Supplementary Figure IX. Nuclear localization of YAP is unchanged between Saline, Liraglutide - treated and MK-0626-treated high fat fed, diabetic C57BL/6J mice after surgical induction of pressure overload. Arrows represent positive nuclei. Representative images n=3-4/group.

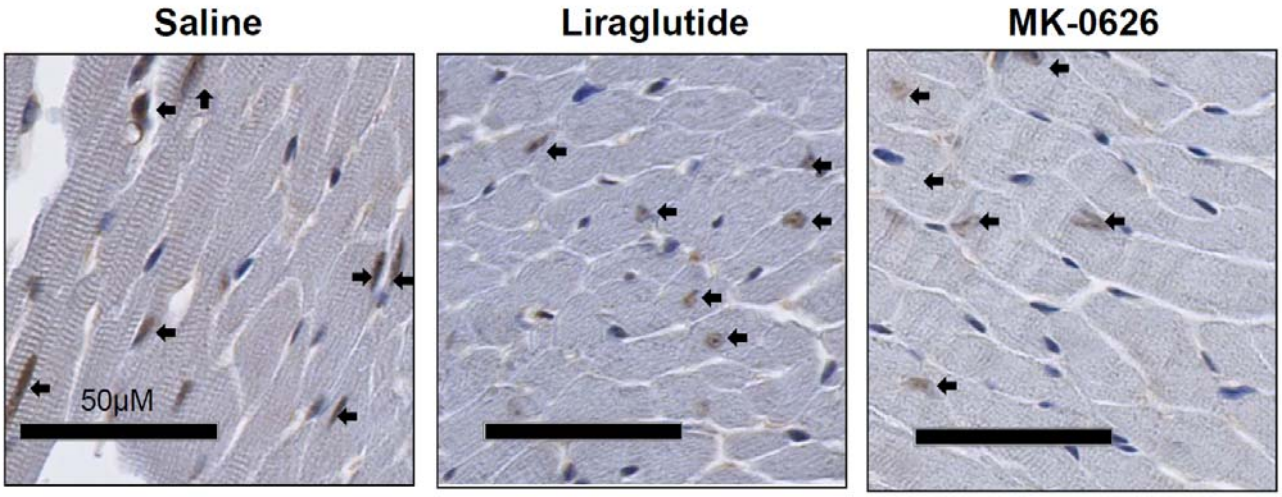

SUPPLEMENTARY DATA

Supplementary Figure X. Treatment with the DPP4i MK-0626 in high fat fed, diabetic C57BL6/J mice after surgical induction of pressure overload has no effect on some markers of inflammation but increases markers of hypoxia. Relative expression of ventricular mRNA levels of **A**: *Il1b*, **B:** *Ccl2* **C:** *Ccl8*, **D**: Gdf15, **E:** *Vim*, **F:** *Hmox1*, **G:** *Vegfa*, **H:** *Nos2*, **I :***Hif1a*, **J:** Nos3 (n≥5 sham group (S) and n=8-13 TAC group (T)). All values are mean±SEM **P*<0.05. ‡*P*<0.05 sham surgery group vs. TAC surgery group.